

Journal Pre-proofs

Review

Recent progress of flexible rechargeable batteries

Xiao Zhu, Haoran Zhang, Yongxin Huang, Er He, Yun Shen, Gang Huang, Shouyi Yuan, Xiaoli Dong, Ye Zhang, Renjie Chen, Xinbo Zhang, Yonggang Wang

PII: S2095-9273(24)00683-2
DOI: <https://doi.org/10.1016/j.scib.2024.09.032>
Reference: SCIB 2973

To appear in: *Science Bulletin*

Received Date: 13 May 2024
Revised Date: 1 July 2024
Accepted Date: 12 September 2024

Please cite this article as: X. Zhu, H. Zhang, Y. Huang, E. He, Y. Shen, G. Huang, S. Yuan, X. Dong, Y. Zhang, R. Chen, X. Zhang, Y. Wang, Recent progress of flexible rechargeable batteries, *Science Bulletin* (2024), doi: <https://doi.org/10.1016/j.scib.2024.09.032>

This is a PDF file of an article that has undergone enhancements after acceptance, such as the addition of a cover page and metadata, and formatting for readability, but it is not yet the definitive version of record. This version will undergo additional copyediting, typesetting and review before it is published in its final form, but we are providing this version to give early visibility of the article. Please note that, during the production process, errors may be discovered which could affect the content, and all legal disclaimers that apply to the journal pertain.



Review

Received 13 May 2024

Received in revised form 1 July 2024

Accepted 12 September 2024

Recent progress of flexible rechargeable batteries

Xiao Zhu^{#[1]}, Haoran Zhang^{#[2]}, Yongxin Huang^{#[3]}, Er He^{#[4]}, Yun Shen^{# [5]}, Gang Huang^{*[2]}, Shouyi Yuan^{*[5]}, Xiaoli Dong^{*[1]}, Ye Zhang^{*[4]}, Renjie Chen^{*[3]}, Xinbo Zhang^{*[2]}, Yonggang Wang^{*[1]}

[1] Department of Chemistry, Shanghai Key Laboratory of Molecular Catalysis and Innovative Materials, Institute of Fiber Electronic Materials and Devices, Collaborative Innovation Center of Chemistry for Energy Materials (iChEM), Fudan University, Shanghai 200433, China.

[2] State Key laboratory of Rare Earth Resource Utilization, Changchun Institute of Applied Chemistry, Chinese Academy of Science, Changchun 130022, China.

[3] Beijing Key Laboratory of Environmental Science and Engineering, School of Material Science & Engineering, Beijing Institute of Technology, Beijing 100081, China.

[4] National Laboratory of Solid State Microstructures, Jiangsu Key Laboratory of Artificial Functional Materials, Chemistry, Biomedicine Innovation Center, Collaborative Innovation Center of Advanced Microstructures, College of Engineering & Applied Science, Nanjing University, Nanjing 210023, China.

[5] National and Local Joint Engineering Laboratory for Lithium-ion Batteries and Materials Preparation Technology, Key Laboratory of Advanced Battery Materials of Yunnan Province, Faculty of Metallurgical and Energy Engineering, Kunming University of Science and Technology, Kunming 650093, China.

These authors contributed equally to this work.

*Corresponding authors.

E-mail addresses: ghuang@ciac.ac.cn (G. Huang), 20210072@kust.edu.cn (S. Yuan), xldong@fudan.edu.cn (X. Dong), yezhang@nju.edu.cn (Y. Zhang), chenrj@bit.edu.cn (R. Chen), xbzhang@ciac.ac.cn (X. Zhang), ygwang@fudan.edu.cn (Y. Wang).

Abstract

The rapid popularization of wearable electronics, soft robots and implanted medical devices has

stimulated the extensive researches in flexible batteries, which are bendable, foldable, knittable, wearable, and/or stretchable. Benefiting from these distinct characteristics, flexible batteries can be seamlessly integrated into various wearable/implantable devices, such as smart home systems, flexible displays, and implantable sensors. In contrast to conventional lithium-ion batteries necessitating the incorporation of stringent current collectors and packaging layers that are typically rigid, flexible batteries require the flexibility of each component to accommodate diverse shapes or sizes. Accordingly, significant advancements have been achieved in the development of flexible electrodes, current collectors, electrolytes, and flexible structures to uphold superior electrochemical performance and exceptional flexibility. In this review, typical structures of flexible batteries are firstly introduced and classified into mono-dimensional, two-dimensional, and three-dimensional structures according to their configurations. Subsequently, five distinct types of flexible batteries, including flexible lithium-ion batteries, flexible sodium-ion batteries, flexible zinc-ion batteries, flexible lithium/sodium-air batteries, and flexible zinc/magnesium-air batteries, are discussed in detail according to their configurations, respectively. Meanwhile, related comprehensive analysis is introduced to delve into the fundamental design principles pertaining to electrodes, electrolytes, current collectors, and integrated structures for various flexible batteries. Finally, the developments and challenges of flexible batteries are summarized, offering viable guidelines to promote the practical applications in the future.

Keywords: Typical structure of flexible batteries; Flexible lithium-ion batteries; Flexible sodium-ion batteries; Flexible zinc-ion batteries; Flexible lithium/sodium-air batteries; Flexible zinc/magnesium-air batteries

1. Introduction

The rapid development of flexible and wearable electronics, including foldable screens, smart watches and roll-up displays, has put high demand on corresponding flexible energy storage systems [1–5]. They not only necessitate high energy density and prolonged cycle life, but also require power sources that can bend and flex without compromising performance or durability, greatly driving the need for advanced battery technologies that are both flexible and resilient [6]. Therefore, an increasing number of researches have been conducted to develop flexible batteries with diverse shapes and sizes to satisfy these applications. Nowadays, the integration of flexible batteries has been successfully achieved into various wearable/implantable devices, catering to the requirements of our daily communications, healthcare monitoring, and smart wearable accessories (Fig. 1). The application domains encompass smart home systems, flexible displays, on-board energy sources and implantable sensors, etc. Step forwards, the unique attributes of mechanical flexibility, high portability, and lightweight nature of flexible batteries are expected to foster new applications in smart skins, epidermal sensors, and even intelligent space suits in the foreseeable future [7,8].

Fig. 1. (Color online) Schematic illustration of the application scenario of flexible batteries.

Different from the conventional batteries that utilize rigid and bulky electrodes, current collectors, metal anodes, liquid electrolytes, and packages, flexible batteries require the flexibility of each component to accommodate diverse shapes or sizes. Hence, it is imperative to design innovative flexible materials and structures that can endure repetitive folding, twisting, and stretching [9]. Accordingly, considerable attention has been devoted by researchers to the development of flexible electrodes and current collectors, along with flexible structures to maintain high electrochemical performance and excellent flexibility [10]. Meanwhile, gel electrolytes have also been extensively investigated owing to their inherent flexibility and low risk of leakage compared to liquid electrolytes during repeated bending or stretching applications. Among these, current collectors act as an important role in supporting the conductivity of active materials and effectively maintaining the flexibility of electrodes, which are generally based on carbon fibers, carbon nanotubes, graphene, and soft metal current collectors. On the basis of these flexible components, batteries with different structures and shapes have been well designed to meet the various device configurations.

Over the past few decades, there has been a significant surge in the popularity of flexible lithium-ion batteries (LIBs) owing to their high energy density and long cycle life. In parallel, other kinds of flexible batteries have also been rapidly developed, including flexible sodium-ion batteries (SIBs), flexible zinc-ion batteries (ZIBs), flexible lithium/sodium-air batteries (LABs/SABs) and flexible zinc/magnesium-air batteries (ZABs/MABs). Although several reviews have made discussions on the topic of flexible batteries, their focuses have predominantly been on the advancements in certain flexible batteries, such as flexible LIBs and flexible metal-air batteries, or specific materials such as graphene and carbon nanofiber [6,10–13]. Obviously, different electrode reaction mechanisms (e.g., air electrodes and metal electrodes in comparison to conventional intercalation compounds) for these batteries have put forward distinct requirements on electrode structures, current collectors, and electrolytes. Therefore, a comprehensive review is urgently

needed to highlight recent advances in different kinds of flexible batteries.

In this review, typical structures of flexible batteries are firstly introduced and classified into mono-dimensional (1D), two-dimensional (2D), and three-dimensional (3D) structures according to their configurations. Subsequently, five distinct types of flexible batteries, including flexible LIBs, flexible SIBs, flexible ZIBs, flexible LABs/SABs, and flexible ZABs/MABs, are discussed in detail according to their configurations, respectively. Meanwhile, related comprehensive analysis is introduced to delve into the fundamental design principles pertaining to electrodes, electrolytes, current collectors, and packages for flexible batteries. Finally, the developments and challenges of flexible batteries are summarized, together with some research directions to promote the practical applications in the future.

2. Typical structure for flexible batteries

Flexible batteries are generally fabricated into different configurations to adapt the practical electronic devices, typically including 1D fiber-shaped structures, 2D planar-shaped structures, and 3D structures as illustrated in Fig. 2. According to variations in electrode and cell configurations, 1D fiber-shaped flexible batteries can be further divided into coaxial type, twisted type, and stretched type [9]. Similarly, 2D planar-shaped flexible batteries can be categorized into unit-film batteries, grid-pattern batteries, and island-pattern batteries [14–16], while 3D flexible batteries can be further classified into serpentine, spine-like, origami, kirigami, and animal-like patterns [17–19]. Among these configurations, 1D and 2D flexible batteries have gained more extensive applications in our daily lives. The utilization of 3D structures is predominantly observed in flexible LIBs, with a limited number of instances reported. Therefore, we will systemically introduce the structures and discuss the characteristics of the 1D and 2D flexible batteries as well as their fabrication strategies in this section, and discuss 3D-structured flexible batteries in the subsequent part of flexible LIBs. Noteworthy, geometric and mechanical parameters are considered as the critical parameters to fairly evaluate the flexibility of flexible batteries, which should be exhaustively assessed when designing a flexible battery [20].

Fig. 2. (Color online) Typical structure of flexible batteries. (a) Coaxial structure; (b) twisted structure; (c) stretchable structure; (d) unit-film structure. Reprinted with permission from Ref. [14], Copyright © 2010, American Chemical Society. (e) Grid-pattern structure. Reprinted with permission from Ref. [15], Copyright © 2011, National Academy of Sciences. (f) Island-pattern structure. Reprinted with permission from Ref. [16], Copyright © 2004, Elsevier. (g) Serpentine structure. Reprinted with permission from Ref. [17], Copyright © 2022, Elsevier. (h) Origami structure. Reprinted with permission from Ref. [18], Copyright © 2021, Wiley. (i) Animal-like structure. Reprinted with permission from Ref. [19], Copyright © 2022, Elsevier.

2.1 1D flexible batteries

The 1D flexible batteries exhibit a fiber-shaped configuration and can be further categorized into three

types based on variations in electrode structures and cell configurations, namely coaxial type, twisted type, and stretchable type. In the subsequent section, we will systematically elucidate the architecture and corresponding examples for 1D flexible batteries.

2.1.1 Coaxial-type batteries

Coaxial-type batteries represent a distinct type of 1D flexible batteries. The two electrodes in a coaxial-type battery are arranged in a coaxial configuration, wherein the electrolyte serves as the interlayer and is wrapped by the outer electrode. The electric field between two electrodes in the coaxial-type batteries is oriented both radially and axially, thereby maximizing the effective electrode area while simultaneously reducing internal resistance. Consequently, the coaxial structure facilitates intimate contact between multiple components, thus minimizing the electrolyte in the devices [21]. The electrophoretic deposition process is commonly utilized for the fabrication of coaxial-type batteries, through which Yadav et al. [22] developed a micro-fibrous LIB comprising of lithium iron phosphate (LFP) cathode, lithium titanate (LTO) anode, and a solid polymer electrolyte (SPE). The battery maintained exceptional electrochemical performance throughout bending tests, underscoring its potential applications for flexible and wearable devices.

2.1.2 Twisted-type batteries

As for twisted-type batteries, two flexible fiber-shaped electrodes enveloped in the electrolyte are wound together with a certain angle to form a double-helix structure. Therefore, twisted-type batteries generally exhibit reduced size, decreased weight, and enhanced flexibility. When the twisted angle of twisted-type batteries approaches zero, the two electrodes are aligned in parallel and the twisted-type batteries are referred to as parallel-type batteries [23]. Wang et al. [24] previously demonstrated 1D flexible Zn||MnO₂ batteries with parallel electrode structure, wherein the MnO₂ cathode was prepared by electrochemical deposition of MnO₂ onto carbon fiber (CF). Subsequently, the flexible Zn||MnO₂ batteries were assembled by separating the MnO₂@CF cathode and zinc wires with glass fiber dipping with ZnCl₂ electrolyte or gel polymer electrolyte. Fang et al. [25] also reported a lithium-sulfur battery using a carbon nanostructured hybrid fiber as the sulfur cathode and lithium wires as anode materials. Owing to the presence of aligned carbon nanotube (CNT) fibers, mesoporous carbon (MC) particles as well as graphene oxide (GO) layers, the fibrous cathode displays decent physical properties and high electrochemical performances. Consequently, the twisted lithium-sulfur batteries sealed in a plastic tube exhibited exceptional flexibility, even when bent or twisted, allowing uniform stress distribution and unaltered open-circuit voltage. Twisted-type batteries can also be assembled by intertwining two fiber electrodes coated with solid-state electrolyte to realize special function. For instance, Sun et al. [26] demonstrated the successful fabrication of a fiber electrode-based supercapacitor that exhibited a self-healing effect. The self-healing twisted-type battery was fabricated by wrapping the aligned multiwall carbon nanotube (MWCNT) sheet around a self-healing polymer fiber and subsequently intertwining such two composite fiber electrodes together.

2.1.3 Stretchable-type batteries

Generally, stretchable-type batteries are fabricated by helically winding the fiber electrodes around an elastic substrate, which is the fundamental component. Based on the central axis property, stretchable-type batteries can be further classified into solid-helix electrode batteries (SHEBs) and hollow-helix electrode

batteries (HHEBs). SHEBs typically consist of a solid central axis wrapped by helical electrodes, forming a spring-like structure. The elastic property of the solid axis is essential for the flexibility of SHEBs. Weng et al. [27] initially employed the lightweight and cost-effective cotton fiber coated with a protective layer of shrinkable tube as the substrate, onto which electrode yarns integrated with CNT were sequentially wound with a gel polymer electrolyte as the separator, to fabricate a high-performance fiber-shaped full battery. Such a SHEB was sealed with an insulated soft package, exhibiting superior tensile strengths compared to individual axis cotton fiber due to the excellent mechanical property of wound CNT.

In contrast to SHEBs, HHEBs are composed of hollow central axis. The hollow-helix structure ensures efficient electrolyte permeability between the separator and electrode, thus enhancing electrochemical performance of flexible LIBs. Kwon et al. [28] fabricated a stretchable anode by electro-depositing Ni-Sn on the copper nanowires, which were then twisted into bundles and subsequently coiled into hollow spiral core. Thereafter, the hollow anode was encased in a tubular outer cathode, constituting a complete HHEB.

2.2 2D flexible batteries

2D flexible batteries generally exhibit a planar configuration and can be further categorized into three types, including unit-film, grid-pattern, and island-pattern batteries. The following section will systematically introduce the architecture of 2D planar-shaped flexible batteries and offer some typical examples to better illustrate the configurations.

2.2.1 Unit-film batteries

Unit-film batteries are typically assembled by sandwiching the flexible cathode, separator, electrolyte, and anode into a planar package, which are relatively easier to fabricate compared to 1D fiber-shaped batteries. Koo et al. [29] demonstrated a thin-film LIB with the aforementioned structure, wherein lithium-phosphorous-oxynitride (LiPON) solid electrolyte was employed to separate the electrodes and the mica substrates were eliminated using a universal transfer method. Owing to the excellent flexibility of both the thin-film electrolyte and electrodes, the thin-film batteries can withstand repeated bending, exhibiting stable cycling retention and rate performance even under different bending angles.

2.2.2 Grid-pattern batteries

Grid-pattern batteries are commonly designed to satisfy the demand of transparent devices. In order to evade the inherent problem of the opacity of electrode materials, a strategy of designing patterned electrodes with small features is usually adopted, thereby ensuring that the nontransparent materials only cover a minimal fraction [15]. In grid-pattern batteries, the opaque electrode materials and metal current collectors beneath are confined within the grid structure, while the rest of the electrode substrate is transparent. Additionally, a flexible transparent polymer electrolyte separates the two electrodes. The flexibility of grid-pattern batteries stems from the utilization of highly flexible transparent substrates, of which the physical properties can be tailored by adjusting the feature dimensions and areal portion of the grid trenches of the electrode. Through this assembly mode, the unpackaged single electrode with a transmittance of 62% in the visible and near-infrared bands, and the gel electrolyte with a transmittance of about 99% synergistically facilitated flexible full batteries with high transmittance of 57%.

2.2.3 Island-pattern batteries

Island-pattern batteries are constructed by interconnecting multiple replicated cells with flexible and stretchable metallization in a specific pattern on the stretchable substrate. In island-pattern batteries, each unit cell is maintained in rigid form to prevent breakage, while being electrically connected by metal interconnect on a flexible substrate. Consequently, island-pattern batteries can accommodate mechanical deformation without loading severe stress on the individual cell unit. Wagner et al. [16] initially brought island-pattern batteries into reality in 2004. In their island-pattern pouch cells, arrays of small-scale unit cells consisting of lithium cobalt oxide (LCO) and LTO as electrodes are interconnected by conducting frameworks with extraordinary stretchable characteristics. Each unit cell was electrically connected by metal interconnects, forming a self-similar serpentine structure at two hierarchical levels. Upon stretching, the second-level serpentine expanded along with the stretching direction, followed by expansion of the first-level serpentine subsequent to the collapse of the second-level serpentine. As a result, the battery exhibited stretchability up to 300% and could be folded and twisted without any discernible reduction in the light-emitting diode brightness [30].

3. Recent progress on flexible lithium-ion batteries

Among numerous flexible energy storage technologies, flexible LIBs assumed a prominent role due to their high energy density and long cycle life. Therefore, this section will present an exhaustive review and discussion on the recent advances and practical applications of flexible LIBs, as well as the challenges impeding their commercial viability. To accommodate diverse device configurations, different structures and shapes have been specifically designed for flexibility, which can be accordingly classified into 1D, 2D, and 3D structures as mentioned above. In order to satisfy the requirements of high flexibility and mechanical deformation, flexible components like soft current collectors and gel electrolytes play a critical role in addressing the limitations posed by bulky and rigid commercialized LIBs. Particularly, the progresses of electrode preparations, cell designs, electrochemical and mechanical performance of flexible LIBs in recent years have been summarized.

3.1 1D flexible LIBs

1D flexible LIBs possess excellent superiority with shapes of fiber or wire, which show unique advantages of miniaturization, adaptability, and weavability [31]. In the past few years, many small and lightweight designs of 1D flexible LIBs have been reported to be capable of deformation into any shape and even available to be wove into textiles [32]. According to different positions of cathode/anode electrodes, electrode structure and manufacturing process, the configurations of 1D flexible LIBs can be classified into coaxial, twisted, stretchable structure and enhanced woven structure by coiling fiber or wire electrodes along with an elastic substrate (Fig. 3a–c) [9].

Fig. 3. (Color online) Progress of flexible LIBs. Schematic illustration of (a) coaxial, (b) twisted, (c) and stretchable 1D LIBs. Reprinted with permission from Ref. [9], Copyright © 2020, Wiley. (d) Schematic of battery cable and lighting of green light-emitting diode (LED) bulb (dim) in different bending conditions.

Reprinted with permission from Ref. [22], Copyright © 2019, American Chemical Society. (e) Photographs of energy-harvesting (textile solar cells), energy-storage (textile batteries), and display textile modules for the all-textile integrated system. Reprinted with permission from Ref. [4], Copyright © 2022, Springer Nature. (f) Schematics to illustrate the easy integration of individual electrode fibers and batteries into commercial fabrics, and image that demonstrate the weavability of the printed electrode fiber into a woolen glove and the complete integration of a full battery into textile fabrics. Reprinted with permission from Ref. [33], Copyright © 2021, Elsevier. (g) Schematics for the one-pot hydrothermal synthesis, and features of freestanding films. Reprinted with permission from Ref. [40], Copyright © 2022, Elsevier. (h) Schematics of the 3D-printing process of self-standing electrodes. Reprinted with permission from Ref. [44], Copyright © 2022, Elsevier. (i) Suitably patterned stretchable electrodes fabricated by 3D printing. Reprinted with permission from Ref. [45], Copyright © 2020, Elsevier. (j) Fabrication of the fiber LIB with polymer gel electrolyte inspired by Boston ivy. Reprinted with permission from Ref. [8], Copyright © 2024, Springer Nature.

Primarily, the architecture of coaxial structure is generally the flexible outer and inner electrode wrapped between a separator to form fiber-type and cable-type batteries. Their unique and excellent mechanical properties might have great potential in portable and wearable electronics. From this, Yadav et al. [22] designed and fabricated a multilayered coaxial structure of micro-sized fibrous solid-state LIBs (Fig. 3d). Benefitting from the high surface area and electrical conductivity, the highly flexible and bendable CF serves effectively as a flexible current collector. Consequently, the assembled 1D fibrous LIBs are highly flexible and can operate under different deformation states. The cost-effective electrophoretic deposition and dip-coating method was applied to fabricate the LFP cathode and LTO anode coated on the CF substrate, which were separated by a polyethylene oxide (PEO)-based solid polymer electrolyte. The as-produced fibrous batteries exhibited excellent flexibility and bendability, which has been further designed and fabricated into a cable battery with multiple bending degrees. The single fiber battery retained 85% of the initial capacity after 100 cycles and showed comparable energy and power density of $\sim 0.006 \text{ Wh cm}^{-3}$ and $\sim 0.0312 \text{ W cm}^{-3}$, respectively. Moving a further step, Liao et al. [4] devised an industrial-scale solution-extrusion method featuring three-channels to continuously fabricate parallel cathodes and anodes encapsulated by electrolyte, which can be used to directly produce fiber batteries in one step. The following full fiber battery demonstrated excellent specific capacity of 86 mAh g^{-1} at a current density of 50 mA g^{-1} and stable charge/discharge behavior over 50 cycles with a coulombic efficiency of 93.6%. As a proof-of-concept, the flexible extruded fiber batteries were weaved into textiles and incorporated within the interior of a tent, which can be charged by the outer layer of solar cells (Fig. 3e).

Besides, the more compact and light-weight twisted structure of flexible LIBs exhibits good weavability, while maintaining stable interfaces across different shapes, diameters, lengths, and moduli of the electrode. The liquid electrolyte could be directly injected to fill the gaps among electrodes, which is more suitable for large-scale fabrication of flexible/wearable electronics. Praveen et al. [33] reported an ink-writing-based 3D printing technology to make electrode fibers, which were then twisted into yarn-structured LIBs. To obtain the desired fiber electrode, $\text{LiNi}_{0.6}\text{Co}_{0.2}\text{Mn}_{0.2}\text{O}_2$ (NCM622) cathode and natural graphite-based ink were prepared and optimized to print on an integrated conductive matrix of vapor-grown carbon fibers and

polyvinylidene fluoride binder (Fig. 3f). The as-assembled fiber batteries with gel electrolyte exhibited excellent electrochemical performance and flexibility with adequate weavability. The proposed 3D printing method has generated a new route to develop twisted flexible LIBs and facilitated the seamless integration of batteries into commercial fabrics, which demonstrated promising potential for commercialization in consumer devices.

Unfortunately, the practical implementation presents a formidable challenge of fabricating batteries such as fiber LIBs with diameters ranging from tens to hundreds of micrometers to easily weave them into wearable and breathable textiles. The internal resistance of fiber-type batteries increased sharply along the length of fibers, thereby substantially compromising the electrochemical performance and limiting the development of high-capacity long fiber batteries. Intrigued by this, He et al. [5] established an equivalent circuit model to systematically investigate the impact of length on battery resistance and demonstrated a hyperbolic cotangent function relationship between internal resistance and fiber length. Based on the systematic studies, they produced meters of high-performance fiber LIBs through an optimized scalable industrial process. Interfacial adhesion is another challenge of high-loading, robust and homogeneous electrode coating on the curved fiber surface. To address this issue, a certain percentage of binders have been optimized to obtain uniform fiber electrodes that remained intact without peeling or cracking even after 100,000 cycles of bending test. The mass-produced fiber batteries delivered an energy density of 85.69 Wh kg⁻¹ and excellent stability of 90.5% capacity retention after 500 cycles. In addition, the produced fiber batteries have been woven into textiles and incorporated into a health management jacket for real scenarios, thereby demonstrating high potential for large-scale application in flexible electronic devices.

Despite that the 1D flexible LIBs generally show high flexibility and can be woven into comfortable textiles compatible with wearable designs, the incorporation of fiber devices with highly curved surfaces poses great challenges in terms of integration methods for practical applications. To address the challenges, Zhang et al. [34] outlined a novel manufacturing process for fabricating twisted fiber electrodes that can be woven into threads for large-scale textile integration. Weaving twisted threads into textiles offers abundant interlaced points for rapid and efficient electrical interconnection, while preserving the breathability of the textile and providing a stable interface and good flexibility. As-fabricated textile systems exhibit exceptional flexibility and robustness, offering distinct advantages over conventional techniques such as printing and sintering that compromise flexibility and cause weak connection strength of fiber-based electronic devices. The stable interface and high flexibility of the designed twisted thread enable the workability of the electronic textiles in wearable devices, such as displays, health monitors, and energy storage systems. More importantly, the entire procedure can be completed within a span of approximately 10 d and is easily reproducible, promoting a further step to fabricate practical energy and electronic devices.

3.2 2D flexible LIBs

2D flexible LIBs, generally in a planar appearance, have been widely developed for soft electronics owing to their high bendability, stretchability and even transparency. They can be fabricated by stacking all component layers into a sandwich structure, or confining two grid-patterned electrodes on a transparent substrate with a transparent electrolyte, or interdigitating positioning anodes and cathodes on the same plane to form a coplanar configuration. For instance, Zeng et al. [35] designed an integrated thin-film structure by assembling all cathode, anode, graphene current collector, and polyvinylidene difluoride (PVDF) electrolyte

together onto the commercially available paper. Subsequently, the fabricated LFP/LTO integrated structure was charged/discharged in the coin cell, which exhibited excellent stability and delivered a capacity of 110 mAh g⁻¹ after 140 cycles at 50 mA g⁻¹. Furthermore, the pouch-type flexible LIB was constructed and packed with polyethylene (PE) film, demonstrating excellent structural stability under 100 times repeated bending tests. Chen et al. [36] introduced a fully integrated thin-film design of a stretchable solid-state lithium-ion full battery, encompassing all stretchable components including electrodes, electrolyte, current collector, and packaging. Primarily, the stretchable current collector was fabricated from the flexible carbon-polymer composite substrate and further coated with a conductive layer of Ag microflakes. The electron percolation path was enabled by Ag flakes in an unstretched state and bridged CNT/carbon black (CB) network under stretching. Accordingly, the current collector exhibited excellent conductivity retention when subjected to different strains ranging from 0 to 100% and repetitive stretching, which indicated its feasibility for flexible batteries. Furthermore, cathode and anode materials were cast on the flexible and stretchable current collector by spray-coating process. The assembled batteries functioned well when stretched, bent, or even twisted, showcasing the suitability under mechanical stress.

To prepare 2D electrodes, active materials of cathode and anode could also be *in-situ* grown on the surface of flexible carbon cloth to form binder-free electrodes [37–41]. Lin et al. [38] achieved *in-situ* growth of MoS₂ nanosheets on carbon fiber cloth with surface-anchored SnS₂, which demonstrated stable structure and high lithium ion/electron conductivity. Based on this binder-free anode, a highly flexible battery using LCO cathode was fabricated and showed desired mechanical flexibility. The *in-situ* growth of the hydrothermal method offers great versatility in design and architecture of flexible electrodes with different morphologies of nanoscale active materials, which has been extensively studied and achieved excellent electrochemical performance and flexibility. Different from the complicated preparation of flexible substrates and electrodes, Kim et al. [40] reported the fabrication of a freestanding electrode film by one-pot hydrothermal synthesis. The as-prepared MnO₂/graphene film showed uniform porous structures and controlled thickness, which could provide abundant channels for the transportation of lithium ions and alleviation of the stress caused by largely volume expansion during charge/discharge (Fig. 3g). Besides, the high specific capacity of α -MnO₂ and robust porous structure enabled the flexible anode with excellent stability after 400 cycles. Despite these, optimization of electrode mass loading is necessary to find the trade-off between electrochemical performance and flexibility. Based on this, Zhou et al. [37] applied a facile solvothermal reaction to synthesize carbon-coated TiNb₂O₇ anode with high mass loading on flexible carbon cloth, reaching a maximum of 10 mg cm⁻². In particular, the 3D nanosheets enabled the anode to achieve superior power performance and excellent cycle stability after continuous bending tests. The fabricated full cell with LiNi_{0.5}Mn_{1.5}O₄ (LNMO) cathode and the synthesized flexible anode showed a high energy density of 130 Wh kg⁻¹ at a high discharge power of ~1800 W kg⁻¹ and displayed a maximum of 229 Wh kg⁻¹ at 100 W kg⁻¹. The battery was effectively stabilized to power the LED indicator under critical bending angles cycling, which demonstrated the desired flexibility and stretchability for wearable devices.

Nevertheless, the soft hydrothermal method needs operation at high temperature and pressure, leading to high risk and cost for mass production, calling for a simple and low-cost manufacturing process for practical applications. Bubulinca et al. [42] developed a simple binder-free method to fabricate flexible self-standing cathodes with commercially available materials. Specially, ball milling was initially introduced to reduce the size of lithium manganate (LMO) particles, followed by ultrasonication to obtain dispersion of

LMO/CNT in aqueous solution of Triton X-100. Subsequently, vacuum filtration was carried out on the PVDF membrane to eliminate the solvent, and finally, a binder-free and flexible LMO/CNT layer was obtained by peeling from the membrane after drying. The uniformly distributed CNT matrix enabled the prepared electrode with good electrical conductivity and stretchability. Scanning electron microscope (SEM) images demonstrated the “island-bridge” structure connecting all LMO materials together. As expected, the self-standing LMO/CNT displayed high electrical conductivity of 46 S m^{-1} and good cycle stability with capacity retention of 93% after 120 cycles at 0.6 C. Li et al. [43] reported a flexible and binder-free silicon-based film composited of Si@SiO₂@carbon nanofiber (CNF) composite by electrospinning method, which could be directly utilized as a free-standing anode with a significantly simplified electrode fabrication process. The utilization of Si anode of high capacity is beneficial to fabricate flexible batteries with high energy density. Moreover, the core-shell structure of Si@SiO₂ spheres could largely suppress the volume expansion of Si, which was further combined with polyacrylonitrile (PAN) fiber to form a cross-linked and 3D porous conductive structure, facilitating faster electron and ionic transportation. As a result, the prepared Si@SiO₂@CNF anode containing 29.6% Si exhibits superior stability and desired flexibility under various bending conditions, which can deliver a high capacity of up to 903.7 mAh g^{-1} after 100 cycles at 100 mA g^{-1} .

Furthermore, specific shape and size of flexible LIBs are usually demanded to meet the diverse factors and complex structure of wearable devices. Benefitting from the distinctive capability to fabricate customized electrode architecture, 3D printing technology has garnered great attention for battery production. Praveen et al. [44] reported an extrusion-based 3D-printing technology to fabricate the self-standing and flexible electrodes. Vapor-grown carbon fibers (VGCFs) were incorporated into electrode ink formulation to enhance the electronic conductivity as well as the function of the current collector, resulting in a trade-off between electrochemical performance and flexibility (Fig. 3h). Tensile strengths and the electrical conductivity of the printed $\text{LiNi}_{0.8}\text{Co}_{0.15}\text{Al}_{0.05}\text{O}_2/\text{VGCF}$ electrode have been comprehensively investigated, which delivered desired flexible property and charge/discharge behavior. Moreover, a prototype pouch cell was assembled using the self-standing electrode and commercial carbonate-based electrolyte, which was stable enough to keep the red LED illuminating under an extremely flexed state. Accordingly, this self-standing electrode design and 3D printing technology offered a pioneering approach to the mass production of flexible LIBs, which are in high demand for customized wearable electronics applications.

3.3 3D flexible LIBs

In addition to the widely investigated 1D fiber-shaped batteries and 2D planar flexible batteries, some unique 3D interdigitated configurations have also been developed to meet various demands in terms of the shape and size. 3D structural flexible batteries have been reported including serpentine structures, spine-like, origami, kirigami and animal-like patterns [12,45–48]. Some emerging composite 3D flexible electrodes and membranes have also been proposed for the development of 3D flexible batteries [49–56]. To prepare deformable electrodes, 3D printing is a facile and low-cost manufacturing technique employing direct ink writing, especially suitable for complex geometrical design (Fig. 3i) [45]. The 3D-printed serpentine structure at the component level enabled the battery to accommodate large and repetitive elongations without significantly straining of the electrodes and the separator. Based on this, Bao et al. [46] developed an evolutionary printing approach to fabricate free-standing and customized kirigami electrodes with desirable deformability, which applied inks with regular viscosity and a customized polydimethylsiloxane template.

Benefitting from the customized structure, excellent mechanical properties and electrochemical performance have been achieved. The full cell, composed of the stretched kirigami LFP and LTO electrodes, exhibited a high discharge capacity of $\sim 100 \text{ mAh g}^{-1}$ at 0.3 C after 100 cycles. These printing technologies provided new paths to obtain highly flexible electrodes for the development of wearable electronic devices. This strategy has also been introduced to fabricate other flexible energy storage systems including flexible supercapacitors [47] and ZABs [48].

Promoted by the natural world, numerous organisms from animals to plants have evolved distinctive structural and compositional properties over billions of years, which confer them with high deformability, robustness, and flexibility [8,57,58]. Inspired by these biological characteristics, numerous innovative designs of flexible LIBs have been proposed. Bao et al. [57] created an overlapping structure of flexible LIBs, comprising hard energy storage scales based on $\text{LiNi}_{0.5}\text{Co}_{0.2}\text{Mn}_{0.3}\text{O}_2$ (NCM523) cathode, graphite anode and bendable connected dermis. The novel overlapping rigid-supple integrated architecture allowed convenient stacking of long electrode strips, enabling high active materials loading of scale parts and flexibility of soft dermis connection. The fabricated prototype battery demonstrated a high volume energy density of 374.4 Wh L^{-1} and exceptional stability barely without capacity degradation under over 11,300 times *in-situ* dynamic bending tests. Recently, Lu et al. [8] designed channel structures in electrodes to incorporate polymer gel electrolytes and establish intimate and stable interfaces for high-performance wearable batteries inspired by the winding characteristic of Boston ivy. In the channel structure, multiple fiber electrodes were rotated together to form aligned channels, while the surface of each fiber electrode was designed with networked channels (Fig. 3j). The monomer solution was effectively infiltrated along the aligned channels and subsequently into the networked channels at first, where the monomers were then polymerized to produce a gel electrolyte and form intimate and stable interfaces with the electrodes. The resulting fiber LIB demonstrated excellent electrochemical performances and could be produced with a high rate of 3600 m h^{-1} per winding unit. Additionally, the fiber LIB textiles were resistant to washing and abrasion, and could work safely under extreme conditions, such as temperatures of -40 and $80 \text{ }^\circ\text{C}$ and a vacuum of -0.08 MPa . Additionally, drawing inspiration from natural organisms that leverage their inherent self-healing capabilities to restore functionality and extend lifespan, several functionalized solid polymeric electrolytes have been proposed as a means to augment battery safety [59–61]. These nature-inspired overlapping structural strategies provide a substantial way to broaden the versatility of flexible LIBs for potential application in more intricate robots engineering.

4. Recent progress on flexible sodium-ion batteries

In the above section, we have introduced recent progress of flexible LIBs. Compared to LIBs, SIBs exhibit enhanced safety profiles, rendering flexible SIBs more suitable as power sources for wearable and implantable electronic devices. SIBs have been regarded as a mature energy storage system with low cost and abundant resources [62]. To overcome the challenges of sluggish kinetics and serious volume deformation caused by the larger ionic radius of sodium ions compared to that of lithium ions, the composition design [63], structural optimization [64], surface modification [65], and morphological control [66] of electrode materials and electrolytes have been carried out simultaneously. Flexible designs have attracted widespread attention and in-depth studies due to their novel route to attain high energy density, high power density, and good adaptability [67]. In this section, we will discuss the advances of flexible electrode

materials, flexible electrolytes, and flexible SIBs, considering their special synthetic methods and assembly processes. Meanwhile, the application and challenge sections for the development of flexible SIBs are proposed.

4.1 Recent progress of electrodes for flexible SIBs

4.1.1 Cathodes for flexible SIBs

Generally, the free-standing method is preferred over the conventional slurry-casting method for fabricating electrode materials, which can be used as both current collectors and conductive pathways [68]. Therefore, various carbonaceous substrates, such as graphene, reduced oxide graphene (rGO), CNTs, CNFs and carbon cloth, as well as metal substrates, such as copper, titanium, and nickel foils are commonly used as scaffolds for the autonomous growth of active materials [69]. Subsequently, the electrochemical performance of flexible cathodes and anodes are discussed according to the diverse synthetic methods. The selection of synthesis routes must comply with the intrinsic characteristics of the materials, considering both mechanical and electrochemical properties.

Representatively, layered metal oxides, polyanionic compounds, Prussian blue analogs (PBAs), and organic compounds (OCs) are feasible cathodes for SIBs, which can also be fabricated into flexible electrodes for flexible SIBs [70]. Due to the different synthetic routes, the high-temperature quenching method is usually carried out during the preparation processes of layered metal oxides and polyanionic compounds, while the room-temperature co-precipitation method is employed to attain PBAs and OCs. Hence, several mild post-processing methods were proposed to achieve free-standing cathodes with high temperature intolerant property for flexible SIBs, such as vacuum filtration [71], electrospinning/electrospraying [72], and hydrothermal method [73].

As shown in Fig. 4a, the fabricated rGO/Na_{2/3}[Ni_{1/3}Mn_{2/3}]O₂ free-standing composite based on the ultrasonic dispersion and vacuum filtration methods exhibited enhanced electrical conductivity and good flexibility, which can be ascribed to the strong π - π bonds between substrate and active materials [74]. Moreover, a free-standing film composed of Na_{2+2x}Fe_{2-x}(SO₄)₃ nanoparticles and CNFs delivered superior structural stability during the long-term cycling, owing to the rapid electron/ion transport pathway provided by the porous carbon skeleton and nanotechnology (Fig. 4b) [75]. Amongst, the well-defined CNFs were attained by combining electrospinning and annealing. As to poor-sodium oxide cathodes, a nanoribbon film consisting of V₂O₅·0.34H₂O and MWCNTs has been prepared by the hydrothermal method instead of high-temperature annealing under a low energy consumption and controllable process [76]. The expanded interlayer spacing of the V₂O₅ could facilitate Na⁺ transport kinetic, meanwhile the introduction of MWCNTs can establish a short diffusion pathway for Na⁺.

Fig. 4. (Color online) Flexible cathodes and anodes for SIBs. (a) Assembly process of rGO/Na_{2/3}[Ni_{1/3}Mn_{2/3}]O₂ free-standing composite. Reprinted with permission from Ref. [74], Copyright © 2014, The Royal Society of Chemistry. (b) Assembly process of CNFs/Na_{2+2x}Fe_{2-x}(SO₄)₃. Reprinted with permission from Ref. [75], Copyright © 2016, The Royal Society of Chemistry. (c) Assembly process of

PDA with catechol groups. Reprinted with permission from Ref. [79], Copyright © 2016, Wiley. (d) Assembly process of rGO/hard carbon. Reprinted with permission from Ref. [86], Copyright © 2018, Elsevier. (e) Assembly process, thermogravimetric analysis and cycling performance of biomass hard carbon. Reprinted with permission from Ref. [88], Copyright © 2020, The Royal Society of Chemistry. (f) Assembly process of VG/MoSe₂/N-C. Reprinted with permission from Ref. [92], Copyright © 2017, Wiley. (g) Assembly process of Sn@CNT@carbon paper. Reprinted with permission from Ref. [93], Copyright © 2015, Elsevier.

As a material that does not require high-temperature preparation, PBA nanoframes obtained from the hydrothermal method were further composed with CNTs via a simple filter process to achieve a free-standing film, which exhibited good structural compatibility and rate performance [77]. Certainly, PBA nanoparticles could also directly grow on the conductive carbon cloth via a simple co-precipitation method to form a hierarchical structure with abundant ion/electron transport channels [78]. The preparation of OCs was typically carried out under comfortable synthesis conditions at room or low (<200 °C) temperatures, enabling the fabrication of flexible OCs electrodes through polymerization on conductive substrates or self-polymerization. For instance, polydopamine (PDA) with a catechol group showed a strong adhesion property, which could be used as both electrode and binder material. Based on the chemical polymerization and filter process, a binder-free PDA-based electrode was built without inactive components (Fig. 4c), leading to a high energy density and long cycle life [79]. Similarly, -SO₃Na groups decorated poly(aniline-co-amino benzenesulfonic sodium) was developed according to a chemical oxidative copolymerization method, delivering a stable flexible structure and strong conductivity [80]. Another design approach involved the self-polymerization of PDA on the surface of CNTs to form a free-standing electrode with rapid electron transfer kinetics and stable chemical bond connection [81]. The diversified means for constructing flexible structures could be conducted on the OCs cathodes due to the chemical composition diversity and soft chain-segment composition.

Overall, a carbonaceous matrix with excellent electronic conductivity and superior flexibility is regarded as a promising scaffold. Nevertheless, it is worth noting that the non-extreme synthesis technologies are the key of flexible structure design. Especially for the cathodes, voltage tolerance, material compatibility, active/inactive ratio, and preparation difficulty are all questions that require further reflection.

4.1.2 Anodes for flexible SIBs

For anodes of SIBs, carbonaceous materials, metal chalcogenides, alloy compounds, titanium-based materials, and organic materials have been widely developed in recent years [82]. Owing to the abundant species and various properties, the quantity of design schemes for flexible anodes significantly surpasses that of flexible cathodes. In addition to conventional methods including hydrothermal treatment, electrospinning, and polymerization, a series of novel techniques have been proposed to introduce multidimensional and subtle structures, such as atomic layer deposition (ALD) [83], chemical vapor deposition (CVD) [84], and electrodeposition [85]. Therefore, large-scale preparation is easier to achieve through these methods.

Carbonaceous materials have attracted great attention due to their abundant resources and considerable

capacity, especially in the case of hard carbon (HC) ($\sim 350 \text{ mAh g}^{-1}$). A rGO/HC film prepared by simple vacuum filtration exhibited high capacity and good ductility (Fig. 4d), which could be ascribed to the active rGO as a strong binder and flexible backbone [86]. Similarly, the MXene-HC film obtained by the vacuum-assisted co-filtration method also delivered superior rate capability [87]. MXene demonstrated application prospects as a multifunctional binder, involving high conductivity and excellent electrochemical properties. Macromolecule and biomass materials are feasible precursors to synthesize HC, and thus cellulose and cotton filter papers were simply impregnated with a phenolic resin solution and subsequently thermally treated at $1300 \text{ }^\circ\text{C}$ to form self-sustained HC electrode (Fig. 4e) [88]. The mechanical property and thermal stability of HC have been improved synchronously, while the natural 3D porous structures provided ample spaces for strain release and a large area for electrolyte contact. In addition to HC, nitrogen-doped CNFs or porous graphene film with a conductive network and good structural stability could also be used as high-performance flexible anodes [89,90]. Generally, titanium-based materials (e.g., TiO_2 and $\text{Na}_2\text{Ti}_3\text{O}_7$) can be prepared by the mild liquid-phase methods, which is beneficial for the design of free-standing anodes. For instance, $\text{Na}_2\text{Ti}_3\text{O}_7$ nanowires were epitaxially grown on the carbon cloth substrate under a hydrothermal process, resulting in rapid electron transport and sufficient electrolyte infiltration [91].

Regardless of the material type or preparation method, metal chalcogenides and alloy compounds have shown outstanding advantages. Meanwhile, a high theoretical capacity can be achieved based on conversion or alloy reactions. However, the low electrical conductivity and severe volume expansion may limit their applications, which provide a requirement for flexible design. The typical hydrothermal and electrospinning routes have been employed to attain various free-standing metal chalcogenides and alloy compounds. The sandwiched arrays, composed of vertical graphene (VG), MoSe_2 nanosheets, and N-doped carbon (N-C), were fabricated via coupled hydrothermal and polymerization approaches (Fig. 4f), which presented a dual conductive framework and good volume accommodation [92]. To develop a refined array on carbon paper with a peculiar hierarchical architecture, a combined soaking-CVD method has been carried out to build a free-standing anode of $\text{Sn@CNT@carbon paper}$ (Fig. 4g) [93]. The CNT sheaths were decorated on the Sn nanorods at expected sites, which provided a conductive pathway and inhibited mutual squeezing between Sn particles. To overcome the insolubility of red phosphorus (RP) in common solvents, a physical vapor deposition route was conducted to attain RP@rGO composite film [94]. The firm connection between rGO and RP not only accelerated electron conduction but also accommodated the volume change. As for organic anodes, their flexibility researches are basically consistent with that of cathodes [95].

In brief, a wider range of materials and techniques are introduced into the design of flexible anodes for SIBs compared to that of cathodes. Fortunately, the challenges posed by limited electrochemical performances and diverse functional requirements can be solved by flexible free-standing structures simultaneously.

4.2 Recent progress of electrolytes for flexible SIBs

The flexible electrolyte plays a critical role in the design of flexible SIBs, necessitating a balance between mechanical properties, ion transport capability, and safety performance. According to different material states, electrolytes in SIBs can be divided into three kinds: Liquid, gel-polymer, and solid-state. Considering the risks of leakage and combustion in flexible SIBs, non-liquid electrolytes with a certain mechanical strength such as gel-polymer and solid-state electrolytes have received much attention. From a

solid-state perspective, the suitable electrochemical window and good interface contact are regarded as important factors to evaluate flexible electrolytes. Representatively, poly(vinylidene fluoride-hexafluoropropylene) (PVDF-HFP) copolymer composed of Na⁺ conductive medium is extensively used as a flexible electrolyte, which can confine the liquid electrolyte within cavities to prevent electrolyte leakage [96]. The PVDF-HFP-coated glass fiber (GF) was developed as a separator with excellent adhesion to the electrode/electrolyte interfaces, delivering stable pathways for Na⁺ transport. In addition to surface modification, PVDF-HFP can couple with polyethylene glycol (PEG) to form a self-supporting film, exhibiting exceptional deformability and liquid-retention capability [97]. The weak hydrogen bond interactions between the MXene filler and PEG-PVDF-HFP copolymer further enhanced the structural stability and ionic conductivity. Similarly, poly(methyl methacrylate) (PMMA) dispersed with silica particles was prepared via a solution immobilization route, which possesses optimal conductivity and flexibility at room temperature attributed to the space charge defects around the silica particles [98].

Currently, the combination of inorganic fillers and organic substrates can simultaneously exhibit high ionic conductivity and good mechanical properties. Compared to the solid polymer and composite polymer electrolytes, the inorganic solid electrolytes with a wider voltage window and enhanced safety features can be considered as a prime flexible electrolyte. The 80 wt% Na_{3.4}Zr_{1.9}Zn_{0.1}Si_{2.2}P_{0.8}O₁₂ (NZP), 12 wt% PEO, and 8 wt% *N*-propyl-*N*-methylpyrrolidinium bis((trifluoromethyl)sulfonyl) imide ([Py₁₃]⁺[NTf₂]⁻, IL) was composited to form a high solid-content electrolyte with flexibility, flame-retardancy and high ionic conductivity [99]. The uniformly distributed particles could be obtained via the simple solution pouring method due to the good film-forming properties and fine particle sizes. For glassy Na-ion solid-state electrolytes (GNSSE), their amorphous structure and compressibility are conducive to achieve rapid ionic conduction and thin flexible film [100]. A 0.5Na₂O₂-TaCl₅ solid electrolyte composed of an oxygen-chloride framework exhibited good ductility, which could construct cold pressed particles with no gaps and high stability under high pressure.

Furthermore, some new types of flexible electrolytes have emerged as options for implementation in SIBs. For example, introducing biomimetic materials and technologies can offer novel insights to the design of flexible electrolytes [101]. A non-liquid electrolyte containing biocompatible normal saline and cell-culture medium with absolute security and good adaptability has been applied to the fiber aqueous SIBs. Inspired by the regulatory technology for binding of water and salt in large biomolecules, methylated polyamide has been prepared to hold more salt in hydrogel electrolyte, which is beneficial for the wide voltage window and high ionic conductivity [102]. Notably, it could maintain transparent and stable structure during the modification process of methyl groups.

Generally, the solid-state electrolyte without free-flowing liquid can be used in flexible SIBs, involving polymer, inorganic and hydrogel materials. However, meeting various requirements such as ion conduction, structural deformation, and safety poses a significant challenge for a single component. Therefore, the design of composite electrolytes, leveraging the advantages of different solid-state electrolytes, can be regarded as a pivotal route to achieve flexible device applications.

4.3 Integrated design for flexible SIBs

The integration of electrodes and electrolytes into flexible SIBs not only requires the alignment of

capacity and voltage, but also necessitates robustness to bear mechanical deformation. Frequently, the flexible structures of SIBs can be divided into three kinds: 1D, 2D, and micro-type. Amongst, the 1D structures possess good bending characteristics and weavability, which can be blended with various fabrics. The 1D structures can be further classified as fiber-shaped and tube-shaped corresponding to different assembly modes. The cable model based on the fiber spiral winding is a highly practical method to achieve battery torsion and expansion [101]. The hollow spiral structure of the electrode ensures sufficient electrolyte infiltration and various deformations. While the tube-type flexible SIBs are composed of a hollow Teflon tube, a copper wire, a thin Na band, a separator, a flexible electrode, and a shrinkable tube, which are fabricated in accordance with conventional coin-type cells [103]. This tube-type structure exhibits good bending and stretching abilities, rendering it suitable for wearable devices.

The 2D structures are constructed by the layered stacking of free-standing electrodes and encapsulation with aluminum-plastic film. When the free-standing Sb/rGO and $\text{Na}_3\text{V}_2(\text{PO}_4)_3/\text{rGO}$ were used as anode and cathode, respectively, the flexible pouch-type SIBs displayed a superior mechanical performance, enabling LED illumination even after undergoing various degrees of bending [104]. However, low tensile strength and susceptibility to fatigue are the drawbacks of this structure. Similarly, the carbon fiber cloth loaded cathode and Na foil anode were integrated into the soft-packaged battery, exhibiting exceptional stability even under bending conditions [105].

The micro-type structures are typically prepared via direct ink-writing and bridge-connection design, aiming to achieve the strongest deformability and excellent electrochemical stability. For instance, the micro-type flexible SIB could be assembled by the electrode ink containing $\text{Na}_3\text{V}_2(\text{PO}_4)_2\text{O}_2\text{F}$ (cathode) and $\text{NaTi}_2(\text{PO}_4)_3$ (anode) with 3D conductive networks, along with electrolyte ink with high ionic conductivity, resulting in rapid electron/ion transport in thick 3D-printed electrodes [106]. It is worth noting that appropriate viscosity and rheological properties are the key factors for electrode ink. The 3D-printed porous conductive framework can accommodate mechanical strain and strong interface interaction between flexible substrates and ionic liquid gel electrolytes, which can achieve serial or parallel fabrication of any devices. In principle, a wide range of materials can be formulated into electrode inks through a reasonable solution ratio. The 3D-printed SIBs containing of $\text{Na}_3\text{V}_2(\text{PO}_4)_3$ ink and $\text{Cu}_2\text{S}@Z\text{nS}/\text{C}$ ink released a considerable energy/power density (122 Wh kg^{-1} and 203 W kg^{-1}) [107]. Beyond micro-type flexible SIBs, the 3D printing technology also exhibits a huge application potential to develop large-scale energy storage devices in the future. In brief, the design of device structure and integration methodology plays crucial roles in achieving flexible SIBs with high deformation stability and electrochemical performance. Whether it is 1D, 2D, or micro-type, their compatibility with wearable devices will be the primary focus of future research.

5. Recent progress on flexible zinc-ion batteries

In the above section, we have introduced recent progress of flexible LIBs and flexible SIBs. Although flexible LIBs and SIBs have promising application prospects, their utilization is accompanied by inherent safety concerns arising from the use of toxic and flammable organic electrolytes. Owing to the high safety, eco-efficiency, substantial reserve, and low cost, flexible aqueous ZIBs have long been considered as promising candidates for energy storage devices in wearable electronic applications [108-111]. Given the deformability, flexibility, and ductility of metallic zinc, aqueous ZIBs are regarded as the most favorable choice for flexible batteries. Moreover, metallic zinc possesses low redox potential (-0.76 V vs. standard

hydrogen electrode), high theoretical capacity, and excellent stability in air and water [112–114]. Consequently, flexible ZIBs have been extensively investigated and are anticipated to power the wearable electronics. In the subsequent section, we will introduce some recent advances in flexible ZIBs by categorizing them into 1D and 2D flexible aqueous ZIBs.

5.1 1D flexible aqueous ZIBs

Based on the battery structures discussed above, 1D flexible aqueous ZIBs can also be classified into three types including coaxial structure, twisted structure, and stretchable structure. Over the past several years, various 1D flexible batteries with different structures have been demonstrated by many research groups [115–121]. 1D ZIBs have recently garnered global attention due to their unique advantages such as low cost, abundant reserves, and environmental friendliness. In order to make 1D flexible ZIBs with high flexibility, all the constituents of flexible batteries, including current collectors, cathodes, electrolytes, anodes, and packages, need to possess exceptional flexibility. Typically, the flexible cathodes of 1D ZIBs are fabricated by depositing active materials onto 1D flexible current collector, such as carbon nanotubes or carbon nanofibers. In addition, conventional liquid electrolytes are susceptible to leakage when subjected to repeated deformation. Therefore, the electrolytes in most of the flexible ZIBs are polymer electrolyte or gel polymer electrolyte [115,116]. Besides the flexible cathode and gel electrolyte, the zinc anode is another challenge that hinders the practical application of flexible ZIBs. Although metallic zinc exhibits a certain degree of flexibility and resilience, it will ultimately succumb to fracture under repetitive deformation. Moreover, the growth of zinc dendrites poses another handicap for the practical application of zinc metal in flexible batteries. Therefore, designing a highly flexible zinc anode with robustness and stability is also imperative. Conventionally, electrochemical deposition or molten diffusion of metallic zinc into the flexible or stretchable conductive carbon fiber is the typical approach.

As depicted in Fig. 5a, Zhu et al. [117] presented a 1D flexible fibrous Zn||Ag battery comprising AgCl cathode, zinc metal anode, and gel polymer electrolyte modified with GO. To improve the flexibility of the proposed Zn||Ag batteries, the AgCl cathode was deposited on the carbon cloth while the zinc anode was deposited on the copper foam. These components were subsequently assembled into a 1D fibrous battery with a thickness of 2.27 mm, forming a parallel electrode structure. GO was incorporated into the gel polymer electrolyte to improve the electrochemical performance, while its amount affected the mechanical properties of the gel. Small amount of GO could improve the tensile strength by promoting strong intermolecular interactions between poly(vinyl alcohol) (PVA) chains and GO. Consequently, the wearable aqueous ZIBs could effectively operate under practical conditions with different deformations. The battery exhibited a slight capacity decrease as the bending angle increased, while maintaining a capacity of 1.4 mAh at a bending angle of 135°, which corresponded to 95.3% of the initial capacity.

Fig. 5. (Color online) 1D flexible fibrous ZIBs. (a) Schematic illustration of fibrous Zn||Ag batteries with GO modified hydrogel electrolyte and electrochemical performance under bending conditions. Reprinted with permission from Ref. [117], Copyright © 2024, Elsevier. (b) Schematic illustration and capacity retention of twisted Zn||AgCl batteries. Reprinted with permission from Ref. [118], Copyright © 2022, The Royal Society of Chemistry. (c) Schematic illustration of LM@Zn metal anode and stretchable ZIBs. Reprinted

with permission from Ref. [120], Copyright © 2024, Wiley. (d) Schematic illustration of the fabrication process of stretchable eG/P-Zn@SFB, bio-inspired design of eG/P-Zn@SFB and integrated device. Reprinted with permission from Ref. [121], Copyright © 2021, American Chemical Society.

Besides parallel electrode batteries, 1D flexible Zn||Ag batteries can be fabricated with twisted structure. Li et al. [118] presented a 1D flexible quasi-solid-state Zn||Ag battery with twisted structure using a gel electrolyte, in which binder-free cathode carbon nanotube fibers (CNTF)-LiNi_xCo_yAl_{1-x-y}O₂ (NCA)-Ag was prepared by directly growing Ag nanoparticle on CNTF with an N-doped carbon conductive scaffold, while zinc metal anode was also deposited onto the CNTF (Fig. 5b). The subsequent cyclic voltammetry (CV) analysis of these batteries exhibited consistency with the aqueous electrolyte-based batteries with same electrodes, indicating analogous redox reaction. The charge/discharge profiles of the batteries demonstrated minimal variation even when subjected to different bending angles ranging from 0° to 180°, highlighting their outstanding flexibility. Moreover, a specific capacity retention of 89% could be achieved after 600 cycles under bending, indicating the favorable bending stability of the devices.

In addition to modifying cathode materials, much attention has also been paid to the design of flexible zinc metal anodes for flexible ZIBs. Typically, flexible zinc anodes are fabricated through the deposition of zinc onto flexible carbon nano-fiber or carbon cloth substrates. The utilization of these highly flexible substrates enhances the flexibility of metallic zinc. Pu et al. [120] reported an intrinsic stretchable fibrous liquid metal@zinc (LM@Zn) anode for stable ZIBs. The flexible zinc metal anode is prepared by coating metallic zinc with liquid metal indium-gallium alloy. The liquid and self-healing properties of LM could significantly improve the flexibility and stretchability of the 1D flexible ZIBs (Fig. 5c). Consequently, aqueous fibrous ZIBs have been assembled by employing a V₂O₅@C fiber cathode and LM@Zn anode with a parallel electrode structure, maintaining remarkable capacity retention of 92.5% after 600 cycles. Moreover, when the stretchable fibrous ZIB was assembled by wrapping a V₂O₅@C fiber on a LM@Zn fiber, along with the utilization of ZnSO₄/polyacrylamide-chitosan (PAM-CS) hydrogel electrolyte, enhanced electrochemical performance could be achieved. Notably, even after undergoing 300 cycles under a strain of 50%, the aqueous ZIBs still exhibited impressive capacity retention of 83.0%.

Although the above-mentioned stretchable flexible ZIBs can be operated stably under strain, the limited elongation capacity (<400%) hampers their practical applicability. Hence, it is imperative to improve the stretchability. On this basis, Li et al. [121] demonstrated an elastic graphene/polyaniline-zinc@silver fiber-based battery (eG/P-Zn@SFB) with a helical structure. The eG/P-Zn@SFB exhibited ultra-stretching properties and could be stretched to 900% while retaining an impressive capacity of 71%. In the fiber batteries, silver fibers with excellent electrical conductivity ($7.4 \times 10^4 \text{ S m}^{-1}$) and mechanical stability ($38.39 \text{ cN dtex}^{-1}$) were adopted as ideal flexible substrates, and zinc metal and graphene/polyaniline nanosheet were subsequently deposited on them to assemble an all-solid-state flexible fiber battery with helix structure (Fig. 5d). Notably, the substrate could be integrated into a wearable pattern via a knitting technique. As a result, the flexible batteries presented superior stretching ability (>900%) and remarkable performance stability under ultra-stretching conditions.

5.2 2D flexible aqueous ZIBs

In contrast to 1D fibrous aqueous ZIBs, the majority of 2D flexible aqueous ZIBs exhibits a film morphology, typically fabricated by stacking the flexible cathodes, solid-state electrolytes, and flexible zinc anodes within a soft package. Similar to 1D flexible ZIBs, all the components in 2D flexible aqueous ZIBs, including the current collectors, electrolytes, separators, and electrodes, should possess exceptional flexibility and demonstrate resilience against repetitive bending, stretching, and twisting.

To prepare the 2D flexible cathodes for ZIBs, carbon cloth is usually employed as the current collector, which is subsequently immersed in a slurry ink comprising a mixture of active materials, conductive carbon black, and polymer binders. An alternative approach is *in-situ* growth of active materials into the flexible substrate [122]. In addition, conventional liquid electrolytes and separators based on glass fibers are unsuitable for flexible ZIBs due to the inadequate intimate contact between the electrodes during bending and twisting caused by the glass fibers-based separators, as well as the high risk of leakage associated with liquid electrolytes. Consequently, solid polymer electrolytes or hydrogel electrolytes are commonly employed as flexible separators and electrolytes for 2D flexible ZIBs. Besides, the incorporation of a flexible zinc anode is crucial for ensuring the performance of 2D flexible ZIBs. While conventional zinc foil displays the characteristics of flexibility, it is prone to fracture upon repeated bending and twisting. A viable solution entails electrochemical deposition or molten diffusion strategies for depositing metallic zinc onto a flexible substrate [123]. For instance, Wang et al. [124] reported a lightweight and flexible 3D carbon nanofiber architecture featuring uniformly distributed zinc seeds, serving as a flexible host for ZIBs. Owing to the large specific surface area, which effectively reduces the localized current density, as well as the presence of zinc seeds that facilitate successive zinc deposition, a highly reversible zinc deposition could be achieved. In the following content, we will exemplify some recent advancements of 2D flexible ZIBs.

Compared with regular ZIBs, designing highly flexible electrolytes or separators holds significant importance for flexible ZIBs. The electrolytes for flexible ZIBs must possess the ability to endure repeated twisting while effectively preventing any liquid leakage, whereas the generally used flexible electrolytes include hydrogel and gel polymer electrolytes. Liu et al. [125] have recently demonstrated a flexible ZIB with a flexible electrolyte (AMHPL) composed of 2-acrylamide-2-methylpropane sulfonic acid (AMPS), ZnO, 2-hydroxyethyl acrylate (HTA), polyethyleneimine ethoxylated (PEI), and LiCl (Fig. 6a). The AMHPL electrolyte, with anchored $-\text{SO}_3^-$ and $-\text{NH}_3^+$ groups serving as ion distributors, not only enhanced the kinetics of Zn^{2+} transportation but also promoted uniform deposition of zinc. Consequently, the flexible ZIB demonstrated a remarkable specific capacity of 302.4 mAh g^{-1} , along with an impressive capacity retention of 96.3% over 500 cycles. Notably, even under bending, rolling, knotting, and twisting condition, the flexible ZIB still maintained stable energy output. The low-temperature performance of flexible ZIBs is a critical parameter for their practical application. Thanks to the inherent designing flexibility offered by hydrogel electrolytes, the freezing point of them can be reduced to $-70 \text{ }^\circ\text{C}$ through polymer structure design [126,127]. Another anti-freezing hydrogel electrolyte was also reported based on zinc tetrafluoroborate ($\text{Zn}(\text{BF}_4)_2$) and polyacrylamide (PAM) [115]. In this electrolyte, the BF_4^- anions could interact with water molecules by $\text{O}-\text{H}\cdots\text{F}$ to replace the $\text{O}-\text{H}\cdots\text{O}$ between water molecules, inhibiting the formation of ice crystal lattice at low temperature. Therefore, the freezing point of hydrogel electrolyte could be reduced to $-70 \text{ }^\circ\text{C}$, enabling the flexible Zn|polyaniline (PANI) full batteries to undergo various bending states and cycle

at ultralow temperature. Impressively, minimal capacity degradation was observed and the charge/discharge curves remained almost unchanged, suggesting the remarkable adaptability and flexibility of ZIBs at ultralow temperature. The mechanical stability of the hydrogel under repeated deformation is another critical parameter for electrolytes in flexible ZIBs. To realize this, Liu et al. [116] reported an optimal anti-fatigue $\text{Zn}(\text{ClO}_4)_2$ -polyacrylamide/chitosan hydrogel electrolyte (C-PAMCS) for all-flexible ZIBs, which exhibited great mechanical stability. The all-flexible ZIBs were fabricated by sandwiching the C-PAMCS electrolyte between $\text{Cu}_x\text{V}_2\text{O}_5 \cdot n\text{H}_2\text{O}$ cathode and zinc metal anode deposited on styrene-butadiene-styrene block polymer (SBS) substrate decorated with silver (Fig. 6b). The two pairs of cathodic/anodic peaks in CV curves were nearly overlapped at different deformation states, indicating the negligible degradation of performance under various bending angles, which underscore the exceptional mechanical flexibility and reliability of the all-flexible ZIBs.

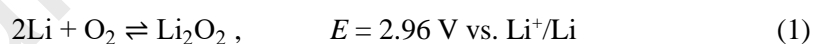
Fig. 6. (Color online) 2D flexible ZIBs. (a) Illustration of preparing the AMHPL electrolyte and VO_{Na^+} cathode for flexible electrochromic ZIBs assembly and application. Reprinted with permission from Ref. [125], Copyright © 2024, Wiley. (b) Schematic illustration of the flexible solid $\text{Zn}||\text{Cu}_x\text{V}_2\text{O}_5 \cdot n\text{H}_2\text{O}$ batteries. Reprinted with permission from Ref. [116], Copyright © 2023, Wiley. (c) Fabrication and characterizations of BH-Zn electrode. Reprinted with permission from Ref. [129], Copyright © 2023, Wiley. (d) The schematic illustration of the preparation process of the 3D printing zinc anode and the electrochemical performances of the assembled full cells. Reprinted with permission from Ref. [130], Copyright © 2023, Elsevier.

In order to enhance the energy density and minimize the size of electronic gadgets, it is critical to optimize the areal capacity of flexible ZIBs, overcoming the limitations in peak performance and production throughput. Yin et al. [128] reported an all-printed polymer-based flexible AgO-Zn battery with ultrahigh areal capacity and low impedance, which were vacuum-sealed in a stacked configuration, using a high throughput, scalable, and layer-by-layer screen-printing process. The flexible AgO-Zn batteries were composed of a multilayered structure comprising nine layers of composite materials. The assembled cells exhibited the highest obtained areal capacity of 54 mAh cm^{-2} for primary applications, with exceptional flexibility and durability under repeated mechanical deformations. In terms of optimizing the flexibility of zinc metal anodes, Liu et al. [129] have reported a biomimetic honeycomb zinc (BH-Zn) anode for flexible ZIBs. The BH-Zn anode was prepared through a series of precise patterning lithography, electrodeposition, nondestructively peeling off, and replacing reaction (Fig. 6c). The optical surface profilometry demonstrated smooth surface and well-organized microholes, favoring the uniform deposition of zinc. The BH-Zn anode, in addition to being superlight and capable of being supported by soap bubbles, exhibited excellent mechanical and electrical stability during operation, which could be attributed to the robustness of the interconnected biomimetic honeycomb structures and the intimate contact of the *in-situ* replaced silver layer. 3D printed technology has also been employed for the zinc powder anodes through direct 3D printing with the 3D print ink comprising carboxylated CNTs, carboxylated CNFs, graphene, silver nanoparticles, and zinc powder dispersed in the deionized water (Fig. 6d) [130]. The well-designed truss-structured zinc anode with regular micro-size pores was fabricated through layer-by-layer stacking of cylindrical strips after 3D printing,

enabling the assembled full cells with stable electrochemical performance under continuous deformation. In addition, a free-standing zinc powder-based anode (ZP-Grad) with gradient particle size and porosity has also been successfully demonstrated as a flexible anode [131]. The ZP-Grad could redistribute the electric field and zinc ion flux, thus effectively suppressing dendrite growth. Therefore, the improved electrochemical performance of ZP-Grad||Na₂V₆O₁₆·nH₂O (NVO) full cell has been achieved, enabling two flexible quasi-solid-state ZIBs in series connection to illuminate the LED board at various bending angles. This further emphasizes the potential application prospects of flexible ZIBs in powering smart and wearable flexible devices.

6. Recent progress on flexible lithium/sodium-air batteries

The rapid development of advanced wearable/implantable electronic devices keeps pursuing high energy density of flexible batteries. Compared to the flexible LIBs and SIBs, metal-air batteries can be expected to realize higher energy density based on the redox reactions of alkali metal anode and oxygen cathode. Both the LABs (~3500 Wh kg⁻¹) and SABs (~1108 Wh kg⁻¹) possess ultrahigh theoretical energy densities, making them promising candidates for next-generation flexible batteries [132–136]. Analogously, through surface and electrode modification, lithium/sodium-sulfur batteries also reveal great potential for practical flexible batteries [137–147]. In the typical discharge process, the alkali metal anode undergoes oxidation into ionic state, while concurrently, gaseous oxygen dissolved in the electrolyte captures electrons on the air cathode to form reduced oxygen species (ROs). Once the metal ions combine with the ROs, solid discharge products would be generated on the cathodes in LABs/SABs. In the following recharge process, these discharge products will decompose backward to the gaseous oxygen, concomitant with the deposition of metallic Li/Na [148–150]. In terms of LABs, the dominant discharge product is Li₂O₂, while NaO₂ is considered to be the main discharge product in SABs due to its superior thermodynamic stability compared to LiO₂ [151]. Generally, the reaction mechanisms of LABs and SABs can be delineated as follows:



At present, impressive advancements have been achieved in improving the electrochemical performance of LABs and SABs, such as cathode material design, electrolyte regulation, and metal anode protection. However, numerous challenges still persist in realizing their practical applications, let alone constructing flexible batteries without compromising the high-capacity advantage [152]. Similar to other types of flexible batteries reported before, the research focus of flexible LABs and SABs includes the air cathode design, electrolyte modification, and metal anode engineering, as well as the design of flexible devices, which will be described in detail in the following parts.

6.1 Progress of air cathode for flexible LABs and SABs

Air cathodes, responsible for the generation and decomposition of the discharge products, exert a profound influence on the performance of LABs and SABs. With the aim of enhancing the oxygen reduction reaction (ORR)/oxygen evolution reaction (OER) kinetics and ensuring the transport of air, high catalytic abilities and porous structures are fundamental prerequisites for air cathodes. Besides, to be applied in

flexible LABs and SABs, the cathodes must exhibit tolerance to bending, wrinkling, and stretching, necessitating a high degree of deformability and mechanical strength. To this end, carbon-based cathodes have garnered significant attention and application in LABs and SABs owing to their facile design of porous structure, low mass density, and high electrical conductivity. By modifying the morphologies and structures of carbon materials, their ORR/OER kinetics and mechanical strength could be improved by establishing unique passages and architectures. Zhu et al. [153] constructed a flexible hierarchical porous graphene foam (HPGF) for flexible LABs, in which the nitrate served as an accelerant for the generation of controllable nano-holes (Fig. 7a). This kind of design endowed the entire air cathode with sufficient mechanical strength and tri-continuous passages for electrons, ions, and oxygen. Consequently, a fivefold increase in the discharge capacity was achieved in flexible LABs. Inspired by the blood capillary tissue, Yang et al. [154] successfully synthesized hierarchical N-doped carbon nanotubes on the surface of stainless-steel meshes (N-CNT@SS) via an *in-situ* growth strategy. This unique structure enabled the cathode with superior electrical conductivity, mechanical strength, stability, and hydrophobicity. Benefiting from these advantageous properties, the assembled cable-type LABs exhibited minimal variation in open circuit voltage when subjected to bending angles ranging from 0° to 180°. Furthermore, the cells also displayed stable cycling stability against a relative humidity (RH) of 43%.

Fig. 7. (Color online) Design of flexible air cathodes, electrolytes, and metal anodes for flexible LABs and SABs. (a) Schematic illustration of the formation mechanism of nano-holes into the graphene layers for HPGF. Reprinted with permission from Ref. [153], Copyright © 2022, Elsevier. (b) Scheme of the preparation process of Ru/LM cathode. Reprinted with permission from Ref. [158], Copyright © 2023, Elsevier. (c) Schematic diagram of a SAB with the structure of sodium foil anode/QPE/air cathode and digital pictures of the LED powered by the integrated flexible SABs at different states. Reprinted with permission from Ref. [161], Copyright © 2020, American Chemical Society. (d) Schematic of the zeolite solid electrolyte, the SSLAB integrated with C-LiXZM, and comparison between the *in-situ* zeolite membrane growth method and traditional preparation method for inorganic solid electrolytes. Reprinted with permission from Ref. [163], Copyright © 2021, Springer Nature. (e) Schematic illustration of the main fabrication processes of OPSP and the hydrogen-bond interaction. Reprinted with permission from Ref. [166], Copyright © 2020, Elsevier. (f) Liquefied pure lithium and Li-Sn hybrid on the stainless steel and copper, and the cross-sectional SEM images of copper fiber coated with pure lithium and Li-Sn hybrid. Reprinted with permission from Ref. [167], Copyright © 2020, Wiley.

Despite the superior properties of carbon-based cathodes, they would experience decomposition under high charge voltage conditions (>3.5 V). Consequently, the development of carbon-free cathodes has been initiated to address this limitation. Jung et al. [155] fabricated carbon-free cathodes with high deformability for flexible LABs by depositing a metallic iridium layer with the outermost IrO_x on the porous and flexible polyimide nanofibers (PI@IrO_x NFs). Due to the great flexibility offered by the polyimide nanofiber structures, the LABs could be assembled in various forms, like pouch, cable, round, and triangle types. Moreover, the pouch/cable LABs exhibited a prolonged operational duration exceeding 60 h with repetitive 300 bending cycles in the ambient air. Besides the air cathodes based on organic substrates, inorganic

substrate-based cathodes have also been designed to further enhance the catalytic efficiency and battery capacity. Cao et al. [156] constructed a self-supporting hybrid film (Ru/Ti₄O₇) by anchoring ruthenium clusters on the Ti₄O₇. The robust interaction between the metal and support facilitated the charge transfer at the interface, coupled with large adsorption energy for the intermediates, enabling the assembled pouch-type LABs with an impressive areal capacity of 5 mAh cm⁻² and a low voltage gap of 0.82 V in the ambient air. Similarly, Guo et al. [157] decorated tellurium nanowires with uniform palladium clusters through a hydrothermal method. This unique structure and composition could promote the homogeneous adsorption and desorption of the discharge products, and reduce the initial dynamical energy barrier for the electrochemical reactions during the discharge process. Consequently, the battery exhibited a long cycling life of 190 cycles and an outstanding specific capacity of 3.35 mAh cm⁻². Recently, Zhang et al. [158] designed ruthenium-decorated GaSn liquid metal composites (Ru/LM) as free-standing flexible cathodes for LABs (Fig. 7b). The incorporation of ruthenium particles into the liquid GaSn resulted in the reduction in surface tension and enhancement in catalytic ability. Accordingly, the pouch-type LABs utilizing the as-fabricated Ru/LM free-standing cathodes could maintain excellent flexibility and were capable of enduring over 95 cycles at a discharge terminal voltage of 2.0 V under the ambient air condition.

6.2 Progress of electrolyte for flexible LABs and SABs

Termed as the blood of a battery, the electrolytes play a pivotal role in ion transport, which drastically influences the performance of batteries. Considering the semi-open operating environment of flexible LABs or SABs, an ideal electrolyte requires good solubility for oxygen and Li/Na salts, strong chemical and electrochemical stability, high ionic conductivity, low volatility, and pronounced hydrophobicity. Among the available solvents, tetraethylene glycol dimethyl ether (TEGDME), distinguished by its high solubility in Li/Na salts and relative stability against ROSs, has been prevalently employed as the electrolyte solvent in LABs or SABs. However, given the significant deformation that the flexible LABs or SABs are likely to undergo during usage, the conventional liquid electrolytes pose a safety risk due to their propensity for easy volatilization and leakage in the semi-open battery systems. To tackle this issue, Liu et al. [159] developed an *in-situ* formed gel electrolyte for flexible SABs through the cross-linking reactions between lithium ethylenediamine and TEGDME. Such gel electrolyte could restrain the H₂O and O₂ crossover, thereby mitigating the corrosion reactions on the anode side. The assembled laminated SABs with this gel electrolyte exhibited robust flexibility and could maintain normal operation under bending, folding, or twisting conditions. Fu et al. [160] also designed a gel electrolyte for flexible LABs. They utilized the gel structure to establish gradient redox mediators (RMs, a type of electron shuttle for reducing the overpotential during the charge and discharge processes) and consequently effectively inhibited the diffusion of RMs, alleviating the side reactions between RMs and lithium anode.

Although gel-type electrolytes have partially overcome the shortages of liquid electrolytes, their mechanical strength remains notably inferior to that of quasi-solid-state or solid-state electrolytes. Wang et al. [161] proposed a quasi-solid-state polymer electrolyte (QPE) that exhibited exceptional performance in flexible SABs. The Na⁺ transfer in the QPE was enhanced by the fluorocarbon chains, leading to a high ionic conductivity of 1.0 mS cm⁻¹. Meanwhile, the QPE with high dielectric constant and hydrophobic properties could induce uniform distribution of Na⁺ on the surface of sodium anode and safeguard the anode against corrosion by atmospheric moisture. As a result, the pouch-type SABs equipped with the QPE could operate

stably for up to 400 h at the arbitrary bending and folding angles (0° – 360°) (Fig. 7c). Additionally, Shu et al. [162] designed a similar electrolyte system to construct flexible LABs, which performed superior safety and stability against extreme treatment.

The utilization of quasi-solid electrolytes could actually improve the electrochemical performance of flexible LABs and SABs to a certain extent. However, the residual liquid component within the quasi-solid electrolytes could still cause some issues, such as poor safety, electrolyte instability, anode corrosion, and dendrite growth. A promising trend lies in the pursuit of solid-state electrolytes, especially those with high ionic conductivity and compatibility towards the lithium/sodium anodes. Chi et al. [163] proposed a kind of lithium-ion-exchanged zeolite X (LiX) zeolite membrane (LiXZM) as the electrolyte for flexible all-solid-state LABs, which showed improved stability, enhanced interfacial compatibility, and high ionic conductivity (Fig. 7d). The dipcoating and wiping seeded growth strategies were applied to ensure the density and homogeneity of LiXZM, so as to facilitate smooth inter-crystal ionic migration. For assembly of the integrated flexible solid-state LABs (SSLAB), the interfaces between LiXZM and cathode/anode were constructed by directly growing LiXZM/molten lithium casting, respectively. Consequently, the SSLABs displayed superior cycling performance compared to conventional aprotic LABs, which could be attributed to the LiXZM-enabled anode protection, modification of discharge products, and inhibition of side products. Furthermore, the SSLABs also exhibited remarkable flexibility, stability, and safety under extreme conditions, achieving a high energy density of approximately 662 Wh kg^{-1} . These outstanding properties offer promising application possibilities for SSLABs, like serving as the power source to drive the stable operation of an unmanned drone.

6.3 Metal anode engineering

Owing to the inherent malleability of lithium or sodium metal, they can be directly used as metal anodes in flexible LABs or SABs. However, it is widely acknowledged that the moisture in the ambient air could undergo severe chemical reactions with the elemental lithium/sodium, let alone the potential for direct water contamination in the semi-open LABs and SABs systems. The application of an artificial layer covered on the anode is an efficient strategy to protect the metal anodes away from the attack of water in the air. Liu et al. [164] designed a stable hydrophobic composite polymer electrolyte (SHCPE) to serve as both an anode protection layer and a separator for flexible LABs. The SHCPE layer possessed superior hydrophobicity, achieving a water contact angle of 131.2° and demonstrating a strong ability to inhibit water penetration. The outstanding water-proof function of SHCPE was evidenced by the direct water drops on both the SHCPE-coated and bare lithium anodes. Notably, the SHCPE-coated lithium anode remained almost unaffected by the water drop, while the bare lithium anode exhibited violent reactions and severe corrosion. Besides, the SHCPE also presented high chemical and electrochemical stability, rendering it an appropriate choice for behaving as a separator. With the above benefits, the SHCPE-modified LABs exhibited comparable discharge curves in both the air and oxygen atmospheres and demonstrated improved cycling performance, while the LABs with unmodified lithium anodes experienced substantial capacity loss. In addition, a pouch-type flexible LAB was also assembled and showed high stability against extreme deformation, nail penetration, thermal treatment, and even water immersion. Similarly, Ye et al. [165] constructed a sodiated carbon nanotube layer (SCL) to stabilize the sodium metal anodes in fiber-type SABs. The reversible extraction and refilling of Na^+ in the SCL during the striping and plating process of sodium metal enables

homogeneous distribution and transportation of Na^+ , effectively suppressing the dendrite growth. Therefore, the as-fabricated fiber-type SABs exhibited a long-term cycling performance of 400 cycles and high stability against deformation.

Aside from the protection layer on the lithium/sodium anodes, the strategy of incorporating external membranes to resist moisture invasion has been proposed. Zou et al. [166] designed an O_2 permeable membrane (OPSP) capable of blocking the passage of water and electrolyte. The membrane was fabricated through the hydrogen-bond cross-linking between the silanol of silica aerogel and the siloxane of polydimethylsiloxane (Fig. 7e), displaying excellent O_2 -permeability and water resistance. The OPSP-protected flexible LABs could even survive with a stable open-circuit voltage when fully submerged in the water for 30 min. In addition, the ability to suppress the electrolyte volatilization and guarantee the oxygen passage of OPSP made the LABs stably cycle for over 660 h in the ambient air.

While the anode protection effects of artificial layers have been demonstrated, direct modification of the metal anodes presents a potentially more efficient strategy for improving the battery performance. Liu et al. [167] designed a flexible anode for LABs by constructing a Li-Sn hybrid metal structure, which bolstered the mechanical strength of the anode and simultaneously restrained the dendrite growth. Additionally, the Li-Sn hybrid metal could enhance the wettability towards the stainless steel and copper foil, as evidenced by dropping molten Li-Sn on these materials (Fig. 7f). Leveraging this property, the Li-Sn hybrid metal could be integrated with copper in a much better contact to increase the anode structural strength. Based on this improvement, a wire-type LAB was assembled and displayed outstanding flexibility and cycling stability.

6.4 Recent progress of flexible LABs/SABs devices design

While significant advancements have been achieved in improving the individual components of flexible LABs/SABs, the architectural design of flexible devices also plays a crucial role in maximizing the battery capabilities to promote their practical applications. Typically, 1D flexible LABs/SABs with linear structures have been commonly fabricated, like wire and fiber forms. These miniaturized structures could exhibit exceptional adaptability and weavability, which rendered broad application prospects in wearable devices. Zhang et al. [168] developed a type of 1D flexible LABs based on a coaxial-fiber architecture. The lithium metal anode was meticulously shaped into a linear configuration and enveloped by the polymer gel electrolyte at the center of the battery. The aligned CNT sheet was subsequently employed to envelop the electrolyte, followed by the packaging tube to encapsulate the entire structure. The designed fiber-shaped LABs demonstrated a high discharge capacity of $12,470 \text{ mAh g}^{-1}$, along with excellent cycling stability of 100 cycles. More importantly, the electrochemical performance could remain almost unchanged upon bending, making it suitable for integration into textile structures for wearable devices. 2D structure is another frequent design in flexible LABs/SABs, which has a large area-to-volume ratio and thinner thickness, enabling high efficiency in utilizing limited space for multiple components. Typically, the 2D batteries are constructed layer by layer, followed by wrapping packaging materials to form a planar structure. Jaradat et al. [169] constructed sheet-type high-performance flexible LABs by incorporating Fomblin-coated carbon cloth at the cathode side to ensure oxygen transport and prevent external water intrusion, while employing MoS_2 nanoflakes as the cathode catalyst along with InBr_3 redox mediator. The battery was assembled in a multilayer structure, displaying robust structure integrity under flat and bending conditions.

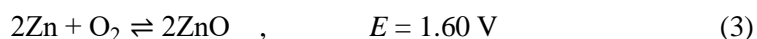
In addition to the dimensional design of the flexible LABs/SABs, the incorporation of solar cells into the batteries to construct self-powered energy systems has recently garnered attention from researchers. Instead of the traditional encapsulation method, the solar-assisted flexible LABs/SABs are packaged within a transparent casing to harness solar irradiation. The integrated energy system has demonstrated superior round-trip energy efficiency and discharge capacity compared to conventional LABs/SABs. For instance, Yang et al. [170] developed a LABs-based flexible self-powered energy system, which integrated commercial solar cells and flexible LABs through a convenient encapsulation method. Under the illumination of solar light, the solar cell functioned as an energy source to power the external devices while simultaneously charging LABs. Conversely, in the absence of light assistance, the LABs behaved in the role of energy output. This work presents a novel and practical approach to designing self-powered systems. Furthermore, in order to directly utilize solar energy, Wei et al. [171] fabricated WSe₂ nanofibers as the free-standing and photoluminescent air cathodes. Under the illumination of visible light, the photocathode increased the specific capacity of LABs from 1.07 to 3.98 mAh cm⁻² at a current density of 1 mA cm⁻², while concurrently reducing the charge/discharge potential gap to 0.49 V. Additionally, pouch-type LABs were assembled with a transparent casing to ensure direct exposure to sunlight, which demonstrated a high areal capacity of 33.03 mWh cm⁻² at a current density of 0.15 mA cm² under illumination and a long cycling lifetime of 120 h with intermittent illumination. Overall, extensive research has been conducted on 1D and 2D structured flexible devices, along with the design of illumination-assisted self-powered battery systems. On the basis of the optimization of the key battery components, the performance of flexible LABs/SABs has received great breakthroughs.

7. Recent progress on flexible zinc/magnesium-air batteries

Compared with flexible LABs/SABs, flexible ZABs and MABs are expected to become the next-generation power sources due to their high theoretical energy densities, biocompatibility, and excellent safety. In contrast to LABs/SABs, which require strictly sealed environment, flexible ZABs/MABs can be directly operated in the air atmosphere. Hence, they are more suitable for fabricating flexible structures. Here in this part, we have comprehensively summarized various flexible battery configurations of flexible ZABs and MABs, followed by some practical applications of flexible ZABs and MABs in multiple fields.

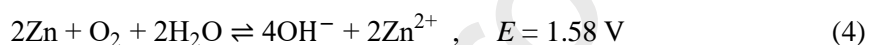
7.1 Flexible ZABs

ZABs stand out as the sole cosmically commercial metal-air batteries attributed to their cost-effective nature, earth-abundant availability, atmospheric stability, unparalleled safety features, and reliability [172,173]. Different from the commonly used organic electrolytes in LABs and SABs, the traditional ZABs generally use an aqueous electrolyte together with a zinc anode and an air cathode [174]. Since the reaction kinetics of ORR and OER are more facile, alkaline electrolytes are typically employed in the system [175]. In alkaline electrolytes, during discharge, O₂ undergoes reduction to OH⁻ through a 4e⁻ or 2e⁻ pathway at the air cathode and subsequently migrates to the zinc anode driven by the potential difference. Simultaneously, the zinc anode is oxidized to Zn²⁺ and combines with the OH⁻ to form Zn(OH)₄²⁻, which subsequently decomposes to ZnO at high concentrations [176]. Therefore, the overall discharge reaction can be represented as follows:



The theoretical energy density should be 1086 Wh kg^{-1} [177]. During the charging process, zinc is reversibly deposited on the surface of the anode, and O_2 is released from the cathode via the oxygen evolution reaction process [178].

Compared to alkaline electrolytes, neutral electrolytes exhibit enhanced environmental compatibility and milder reactivity, thereby mitigating undesired side reactions [179]. Consequently, they have garnered increasing attention in recent years. Different catalysts exhibit distinct electrochemical behaviors in diverse electrolytes, resulting in variations in their operational mechanisms [180]. Briefly speaking, in neutral electrolytes, the reaction path of oxygen electrochemistry is analogous to that in alkaline electrolytes. Due to the lack of OH^- , Zn(OH)_4^{2-} is dramatically reduced, and the coordination of Zn^{2+} depends on the composition of the neutral electrolyte [181]. The theoretical equilibrium potential under neutral condition is slightly lower than that under alkaline condition. Therefore, the overall discharge reaction can be summarized as follows:



Similar to other flexible batteries discussed above, the configurations of flexible ZABs encompass two main types: 1D fiber-shaped and 2D planar-shaped configurations [182]. Accordingly, recent advances in flexible ZABs will be comprehensively elucidated in the subsequent two parts, accompanied by illustrative examples showcasing their practical applications.

7.1.1 Flexible planar-shaped configurations

The fabrication of planar-shaped ZABs is a relatively well-established technique [183]. The typical fabricated structure is a sandwich configuration, with assembly procedures resembling those employed in the production of coin-type batteries [184,185]. The batteries typically consist of flexible electrodes, quasi-state or solid-state electrolytes, and flexible encapsulation materials. As shown in Fig. 8a, a flexible ZAB was assembled with a sandwich structure using Pt/C-RuO₂-loaded carbon cloth as air cathode, zinc foil or zinc-deposited carbon cloth as anode, and microcapsules/hydrogel as electrolyte [186]. The battery exhibited a specific capacity of 758 mAh g^{-1} and excellent rechargeability with stable cycling of 960 cycles and 320 h. Meanwhile, this flexible ZAB presented stable galvanostatic discharge-charge curves under various bending conditions.

Fig. 8. (Color online) Configurations and applications of flexible ZABs. (a) Schematic illustration of flexible ZAB with a sandwich structure, and the galvanostatic discharge-charge curves under various mechanical deformations. Reprinted with permission from Ref. [186], Copyright © 2022, Wiley. (b) Schematic illustration of 800% stretchable planar-shape ZAB. Reprinted with permission from Ref. [189], Copyright © 2019, Wiley. (c) Schematic of the hybrid fiber anode-based ZAB. Reprinted with permission from Ref. [196], Copyright © 2023, Wiley. (d) Schematic depicting how ZABs along with solar cells and sensors were integrated into wearable textiles, and real-time heart rate acquired by a sensor during rest and running. Reprinted with permission from Ref. [201], Copyright © 2023, Wiley. (e) Schematic illustration of the effect of ZAB-based nerve conduit for nerve regeneration. Reprinted with permission from Ref. [205], Copyright ©

2023, Wiley.

Ideal flexible ZABs also need to be stretchable to accommodate strain deformation by substituting rigid components with materials that can incorporate stretchability into batteries [187]. For instance, a flexible metal electrode for ZABs was fabricated by employing a two-step deposition method on polyurethane sponges [188]. In contrast to the conventional electrodes, the flexible substrate imparted softness to the electrode, enabling the assembled ZAB with stable charge/discharge performance even under complex rolling and twisting deformations. Furthermore, the planar ZABs can be designed into many stretchable forms, such as wavy, serpentine, and kirigami patterns. Ma et al. [189] reported an 800% stretchable planar ZAB with a wavy structure, which provided adequate space for stretching by providing abundant wrinkled areas (Fig. 8b). Surprisingly, the maximum output power densities exhibited an improvement as the strain increased. Simultaneously, the discharge voltage plateau moved up while the charge voltage plateau dropped with stretching, resulting in the enhancement of energy efficiency of ZABs, owing to the increased contact areas between active materials and electrolyte.

7.1.2 Flexible fiber-shaped configurations

In comparison to 2D planar counterparts, 1D flexible fiber-shaped batteries exhibit superior adaptability to irregular surfaces such as the human body and possess the knittability to construct textile fabrics [190]. Consequently, there has been a significant surge in research focused on flexible fiber-shaped ZABs. There are several types of fiber-shaped configurations, such as coaxial, twisted, and parallel structures. The coaxial configuration maximizes the gas adsorption area, thereby enhancing the chemical reaction of the battery, which makes itself the predominant structural design to construct ZABs [191]. The coaxial ZABs generally comprise zinc wire anode, electrolyte, and air cathode arranged in concentric layers. For instance, a fibrous ZAB with a coaxial structure was constructed with zinc wire anode, PAM hydrogel electrolyte, rGO-coated CaMnO_3 nanofiber cathode, and heat-shrinkable tube capsulation [192]. The battery was flexible in adapting to various deformations and could be knitted into a hat without destruction. Impressively, it exhibited a high peak power density of 56 mW cm^{-2} and an exceptional cycle life exceeding 80 h at a low temperature of $-40 \text{ }^\circ\text{C}$.

The stretchable fiber-shaped ZABs can also be obtained by structural design. In contrast to planar batteries, fibrous batteries are fabricated into helical spring structures in order to achieve stretchability [193]. Chen et al. [194] demonstrated a 500% stretchable fiber-shaped ZAB consisted of zinc spring anode, virus-like Co-N-Cs air cathode, and hydrogel electrolyte based on sodium polyacrylate and cellulose. The battery demonstrated exceptional electrochemical performance with an energy density of 128 mW cm^{-2} and cycling stability for >600 cycles at the current of 2 mA. Besides, the 500% stretched state broadened the contact areas between the electrolyte and the active materials, improving the electrochemical performance without compromising the battery.

However, the inherent instability of the electrode structure leads to the disintegration of the zinc foil/wire anode, resulting in electrical contact failure. To address this issue, researchers have employed various approaches to construct the anode, including surface modification and utilization of electrodeposited

zinc or zinc powder to fabricate composite electrodes [195]. Chen et al. [196] employed CNT fiber possessing inherent chemical stability and zinc particles with large surface area to design a hybrid Zn/CNT fiber anode with stable structure and high reaction kinetics (Fig. 8c). As a result, the ZAB based on the hybrid fiber anode could be stably charged and discharged for 35 h, dramatically surpassing that of the zinc wire anode. Moreover, the designed fiber ZAB demonstrated high flexibility and stable electrochemical performance under dynamic deformation.

7.1.3 Applications of flexible ZABs

The battery is one of the critical parts of electronic devices that provide energy to ensure normal operation [197]. The emergence of wearable electronics has led to new battery requirements, necessitating flexibility, shape adaptability, high energy density, small size, and high integration [198]. Flexible ZABs possess the potential to fulfill diverse requirements, positioning them as a promising power system for wearable electronics [199]. The high energy density of the flexible ZABs enables devices to operate for more extended periods in limited weight and volume. Meanwhile, unlike conventional batteries with bulky design and configuration limitations, flexible ZABs have the advantage of various geometries for different application scenarios.

Planar-shaped batteries can be used in curved displays, touch screens, wristbands, watches, and even mobile phones [200]. As a typical paradigm, an intelligent wearable system was achieved by integrating solar cells as the energy harvester, planar ZABs as the energy storage part, a wireless charger, and sensors for real-time health monitoring (Fig. 8d) [201]. In this system, the planar ZAB has been transformed into a wristband that serves to power the temperature sensor, wirelessly charge a handheld smartphone, and power a wrist-worn heart rate sensor. The real-time heart rate sensor could operate continuously for approximately 300 s, capturing heart rate variations during rest and running scenarios. Fiber-shaped batteries can be knitted directly into textiles or stitched into existing fabrics [202]. Although attempts have been made to weave the fiber-shaped battery into textiles and successfully power an LED light [203], it remains a significant challenge for practical applications. For instance, they should be thin enough (about 200–300 μm) to meet the weaving/knitting requirements, while the existing fiber-shaped ZABs were generally thick with diameters of millimeters.

In addition, integrating batteries into electronics is also a crucial issue. Future electronic devices must be miniaturized and lightweight, especially for implantable bioelectronics that can significantly reduce implanted areas [204]. For example, an implantable ZAB was integrated into the nerve duct with a minimal volume (0.86 mm^3), which can tightly wrap the damaged nerves and provide accurate *in-situ* electrical stimulation for repairing and regenerating long-segment peripheral nerve (Fig. 8e) [205]. Cell experiments showed that the *in-situ* electrical stimulation provided by the battery promoted the proliferation of Schwann cells and the expression of nerve growth factors. After 12 weeks of treatment, the rats with sciatic nerve injury regained motor function, and the treatment effect was comparable to the “gold standard” of autologous nerve transplantation, without the risks of autologous nerve transplantation.

7.2 Flexible MABs

Compared to ZABs, MABs exhibit superior biocompatibility due to the higher tolerance of magnesium

by human body (Mg: 350 mg d⁻¹, Zn: 9.4 mg d⁻¹) and possess a higher theoretical equilibrium potential and energy density (3.1 V and 2850 Wh kg⁻¹, respectively) [206]. In addition, in contrast to the majority of metal-air batteries, MABs generally use a neutral electrolyte. During discharge, O₂ is catalytically reduced to OH⁻ at the triple-phase boundaries between the air cathode, gas, and electrolyte, subsequently migrating to the surface of the magnesium anode. At the same time, magnesium metal undergoes oxidation to form Mg²⁺, and the coordination of Mg²⁺ is contingent upon the composition of the neutral electrolyte. In most studies, Mg²⁺ reacts with OH⁻ to form insoluble Mg(OH)₂. The overall reactions are as follows:



Different from the rechargeable ZABs, the charging of MABs with the aqueous electrolyte has not yet been achieved, primarily due to the suboptimal thermodynamic and kinetic properties of the discharge products, which hinder the reverse reaction [207]. Meanwhile, the high polarization and the much lower operating voltage compared to the theoretical voltage of MABs, greatly impede the performance. Therefore, the development of flexible MABs is relatively sluggish. Herein, a comprehensive overview of the recent advancements in flexible MABs is presented, which may attract more attention to this research direction.

7.2.1 Flexible planar-shaped configurations

After systematic researches, the planar configurations still dominate the current landscape of flexible MABs [208]. However, the practical application of flexible MABs is still limited by significant challenges, despite their promising prospects. The primary obstacle lies in the deviation between the actual battery performance and its theoretical counterpart. One of the main challenges for cathodes is the sluggish kinetics of the ORR progress [209]. Reinforcing the inherent catalytic activity and implementing innovative electrode designs are imperative for ameliorating the existing limitations [210]. For instance, a flexible 3D hierarchical porous cathode with excellent oxygen electrocatalytic performances was successfully fabricated through the integration of atomic Fe-N_x onto the open mesoporous N-doped-CNFs (OM-NCNF-FeN_x) (Fig. 9a) [211]. The interconnections and 3D layered porous networks of the cathode could significantly promote mass transfer, thereby bolstering electrochemical performances. Consequently, it exhibited enhanced ORR performance compared to CNF-based catalysts reported previously (with *E*_{1/2} values ranging from approximately 0.720 to 0.820 V). The planar-shaped MAB with an OM-NCNF-FeN_x cathode exhibited a higher power density of 5 mW cm⁻², exceeding that of the Pt/C counterpart. More importantly, it could effectively maintain a stable discharge voltage when subjected to significant bending angles (90° or 150°) or folded back to the front, which verified the excellent flexibility of the battery.

Fig. 9. (Color online) Configurations and applications of flexible MABs. (a) Schematic illustration of the ORR progress for OM-NCNF-FeN_x nanofiber catalysts. Reprinted with permission from Ref. [211], Copyright © 2018, Wiley. (b) Schematic illustration of the fiber MAB. Reprinted with permission from Ref. [215], Copyright © 2021, Wiley. (c) Optical images of the batteries mounted onto a human forearm, and the schematic illustration of the sweat-activated MAB. Reprinted with permission from Ref. [219], Copyright © 2022, Elsevier. (d) Future visions for electrical brain stimulation, a voltage-time curve of the pulse power supplied by the brain stimulator powered by an MAB, and EEG signals before and during the electrical

stimulation. Reprinted with permission from Ref. [218], Copyright © 2023, Wiley.

For anodes, the self-corrosion phenomenon of magnesium anode has caused low utilization, sacrificing the actual energy density [212]. Specifically, the spontaneous occurrence of the side reaction ($\text{Mg} + 2\text{H}_2\text{O} \rightarrow \text{Mg}(\text{OH})_2 + \text{H}_2$) suggests direct electron transfer from Mg to H^+ rather than reliance on an external circuit. The optimization strategies primarily encompass anode alloying, anode modification, and electrolyte additives. Song et al. [213] reported a flexible planar MAB employing $\text{Mg}(\text{OTf})_2$ as the electrolyte to mitigate the self-corrosion of the magnesium anode and enhance its utilization efficiency. The improvement was primarily attributed to the spontaneous formation of a protective layer of MgF_2 on the surface of the magnesium anode when immersed in the $\text{Mg}(\text{OTf})_2$ electrolyte, effectively shielding the magnesium surface from water. Therefore, the corrosion rate of magnesium in $\text{Mg}(\text{OTf})_2$ electrolyte was $0.021 \text{ mg cm}^{-2} \text{ h}^{-1}$, exhibiting a tenfold reduction compared to that in NaCl electrolyte. As a result, the MAB had a high utilization of 87.32 % based on magnesium anode compared to that of 44.8 % in NaCl electrolyte. Moreover, the flexible MABs connected in three series successfully powered the sports bracelet with an open circuit voltage of 5.98 V.

7.2.2 Flexible fiber-shaped configurations

As mentioned in the preceding section, 1D fiber-shaped devices exhibit superior knittability for textile construction and adaptability to irregular surfaces. Besides self-corrosion, the magnesium anode suffers from continuous growth of passivation layers derived from discharge products, leading to severe polarization and reduced output voltage [214]. Li et al. [215] proposed a double-layer gel electrolyte to solve the problems of magnesium corrosion and passivation layer formation. The flexible fiber-shaped MAB was assembled by integrating magnesium wire as the anode, MnO_2/CNT sheets as the cathode, and dual-layer gel comprising organic gel and hydrogel as the electrolytes (Fig. 9b). The organic gel effectively shielded the magnesium metal from corrosion, while the hydrogel electrolyte facilitated water supply for the ORR progress in the air electrode. Moreover, the utilization of chlorine salt in the electrolyte resulted in the formation of $\text{Mg}_2\text{Cl}(\text{OH})_3$ discharge product with a distinctive needle-like morphology, which was conducive to the complete contact between the electrolyte and unreacted magnesium-negative electrode. Therefore, the utilization of magnesium in the discharge process was dramatically improved, leading to the high average specific capacity of 2190 mAh g^{-1} and energy density of 2282 Wh kg^{-1} , which was higher than that of the MAB with a single hydrogel electrolyte. In addition to the high electrochemical performance, the battery exhibited remarkable flexibility in accommodating various transformations.

Although the MABs can successfully discharge in simulated humoral environments *in vitro*, their application for implantable purposes remains a formidable challenge. For instance, apart from the inherent problems of MABs, the body fluid harbors a plethora of cells and proteins that can be easily adsorbed/adhered to the implanted batteries, causing the cut-off of O_2 transport [216]. Besides, the implanted batteries are prone to eliciting foreign body reactions [217]. He et al. [218] developed an implantable MAB with both high energy density and biocompatibility. Inspired by the mitochondrion, the battery featured a double-membrane architecture comprising a hydrophobic polymer layer as the inner membrane and a modified phospholipid as the outer membrane. The inner membrane could greatly reduce H_2O permeability,

and effectively mitigate magnesium corrosion, while the outer membrane demonstrated high permeability of O₂ and biocompatibility to ensure continuous O₂ transfer and minimize foreign body reactions. Consequently, it exhibited adaptability to various biological environments, encompassing the brain, abdominal cavity, subcutaneous tissues, and muscles, while demonstrating a high energy density of 2517 Wh L⁻¹ based on the total volume of the battery. Moreover, by employing the double-membrane structure design, the biosafety remained unaffected by the electrochemical reaction of the battery, and the battery could form a seamless integration with biological tissues.

7.2.3 Applications of flexible MABs

Flexible MABs can serve as a superior power source for wearable and implanted electronics, enabling enhanced integration owing to their higher energy density compared to ZABs. Liu et al. [219] demonstrated a soft skin-integrated microelectronics system powered by four planar MABs connected in series, capable of wirelessly and real-time monitoring human health-related signals (Fig. 9c). The battery was a bandage-like device fabricated by using a breathable athletic tape as the substrate and adhesive layer to the skin, a graphene-coated nickel foam as the gas diffusion layer and cathode, a cotton layer containing potassium chloride powders as the separator and electrolyte, a magnesium foil as the anode, and a bottom cotton layer as the separator between anode and skin, exhibiting ultrathin characteristic, flexibility, conformability, sweat-activated feature, high power density (16.3 mW cm⁻²) and impressive energy capacity. When the microelectronics system was worn on the arm during a 1.2-h hike outside at 34 °C, the measured physiological data (including skin temperature and pulse rate) were wirelessly transmitted to the paired cellphone for real-time display. Therefore, it exhibited significant potential in real-time monitoring of exercise performance.

In contrast to wearable applications, implantable batteries necessitate specific criteria including compact size, lightweight construction, high energy density, extended lifespan, exceptionally stringent biosecurity, and the absence of potential leakage [220]. Thanks to the high energy density and biosafety, MABs exhibit significant potential for implantable applications and can be highly integrated with medical devices, enabling previously unattainable *in vivo* miniaturization. He et al. [218] demonstrated the implantable applications of MABs by integrating them into the brain stimulator. The ideal brain stimulator should be sufficiently compact for implantation within the skull or possibly even in a burr hole. This will greatly mitigate the risk of infection and device failure due to extension cable penetration and cable breakage. By using the MABs as the power source, the stimulator could be miniaturized and fully implanted in the skull for *in-situ* electrical stimulation. As shown in Fig. 9d, the miniaturized brain stimulator successfully drove ventricular rapid pacing. It produced electroencephalogram signals ranging from 0.004 to 0.4 mV when a pulsed voltage with a frequency of 3 Hz and pulse duration of 6 s was delivered every 6 s. These compelling results further underscore the potential applications of flexible MABs in future wearable and implanted devices.

8. Summary and outlook

The rapid proliferation of flexible and wearable smart electronic gadgets in our daily lives has stimulated global investigation into flexible batteries, which are deemed as promising power sources for those flexible electronic devices. In this review, we have provided an overview of recent progress of different kinds of flexible batteries, encompassing flexible LIBs, SIBs, ZIBs and metal-air (e.g., LABs/SABs and

ZABs/MABs). To adapt to the practical flexible electronic devices, these flexible batteries are typically fabricated in 1D fiber-shaped, 2D planar-shaped, or 3D structured configurations based on corresponding flexible electrodes, current collectors, and electrolytes. Tremendous efforts have been invested into these flexible batteries, generating significant advances. However, there still exist numerous formidable obstacles hindering the widespread applications of these flexible batteries, which are enumerated as follows:

(i) Further improvements are required in both the specific gravimetric energy density and specific volumetric energy density of flexible batteries, in order to enhance the portability, compactness, and lightweight nature of flexible and wearable electronic devices. Compared to conventional rigid batteries configurations, the energy density of flexible batteries is significantly reduced due to the inclusion of a substantial amount of electrochemically inactive materials necessary for ensuring the flexibility of the batteries. For instance, in 1D stretchable batteries, a stretchable axis that does not contribute to extra capacity is necessary to ensure the flexibility and stretchability of 1D stretchable batteries. Therefore, future endeavors should prioritize the development of novel battery configurations that incorporate fewer electrochemical inactive materials.

(ii) Safety and biocompatibility should be considered given that flexible batteries are primarily utilized in smart and wearable electronic gadgets or implantable electronic devices, which come into direct contact with the human body. Electrochemical systems containing toxic chemical compounds or at risk of explosion are not suitable for fabricating the flexible batteries. Consequently, compared with LIBs, zinc/magnesium-based batteries with aqueous or hydrogel electrolytes exhibit greater potential for the fabrication of flexible batteries. In addition, conventional liquid electrolytes pose a significant risk of leakage or vaporization during the repeated deformation process or in the semi-open metal-air batteries. As a result, solid polymer electrolytes or gel electrolytes, which are nonflammable and leakless, prove to be more suitable for flexible batteries.

(iii) Complicated production procedures and exorbitant costs impede the large-scale production of flexible batteries. Primarily, the design and manufacturing of immature flexible devices result in limited application scenarios. Moreover, production efficiency incurs costs in addition to those of raw materials and equipment. Besides, compared with metal-based current collectors, carbon-based current collectors such as carbon cloth are deemed more appropriate for flexible batteries. Nevertheless, the production cost of carbon cloth exceeds that of conventional metal current collectors significantly. As for the metal-air batteries, the air cathodes are usually established on expensive flexible substrates and loaded with noble metal catalytic materials, posing substantial challenges due to their cumbersome nature and high cost. Meanwhile, the metal anodes need modification to improve stability, which requires external procedures or the use of an auxiliary membrane, bringing additional steps and expenses. Therefore, convenient and scalable manufacturing methods are crucial for the advancement of flexible batteries. Representatively, roll-to-roll printing, electrospinning, 3D printing, magnetron sputtering and chemical vapor deposition have been developed to attain scalable flexible electrodes with high volumetric energy density and firm structure. It is estimable that the integration of electrode materials and substrates can be achieved through these methods, resulting in rapid ion/electron transport and good interface compatibility. However, accurate parameter settings and reduced costs remain the key challenges for application.

(iv) Reliable integration technologies are the determinant for the advancement of flexible batteries. Although

the breakthroughs have been achieved in fundamental theory and key materials, there is still a need for further advancements in integration technologies. The solid-state polymer electrolytes and artificial interfaces with outstanding ionic conductivity and tight connectivity exhibit important effects on device integration. However, the layer-by-layer structure inherently poses mechanical risks. Therefore, the integrative design containing electrode, electrolyte and encapsulant can be regarded as a practical direction for further development. Meanwhile, customized research is imperative to match flexible batteries with wearable devices.

(v) A comprehensive and standardized evaluation system should be proposed for flexible batteries. To date, the assessment criteria for evaluating the flexibility of previous reports have been based on varying bending angles, bending radius, and bending cycles. Such discrepancies in standards make it inappropriate to compare these studies. Therefore, the proposal of a comprehensive evaluation standard, encompassing flexibility parameters and battery size, is in great need for standardized testing and batch production of flexible batteries.

Nowadays, the integration of flexible batteries has been successfully achieved into various wearable/implantable devices, catering to the requirements of our daily communications, healthcare monitoring, and smart wearable accessories. The application domains encompass smart home systems, flexible displays, on-board energy sources and implantable sensors. With further tackling the above issues, the application field of flexible batteries is expected to witness further expansion in the foreseeable future, encompassing areas such as smart skins, epidermal sensors, and even intelligent space suits. At that time, it will become feasible to achieve large-scale and cost-effective fabrication of flexible batteries with the development of printable electronic techniques.

Conflict of interest

The authors declare that they have no conflict of interest.

Acknowledgment

This work was supported by the National Key Research and Development Program of China (2022YFA1203002 and 2022YFB2502102), the National Natural Science Foundation of China (22175086, 22005137, 52204312, U23A20575, and U2130204), Natural Science Foundation of Jiangsu Province (BK20200321), Program for Innovative Talents and Entrepreneurs in Jiangsu (JSSCTD202138), and Yunnan Fundamental Research Project (202301AT070400).

Author contributions

Xiao Zhu contributed in writing, modifying, and revising. Haoran Zhang contributed in writing and reviewing. Yongxin Huang contributed in writing and reviewing. Er He contributed in writing and reviewing.

Yun Shen contributed in writing and reviewing. Gang Huang contributed in conceptualization and reviewing. Shouyi Yuan contributed in conceptualization, reviewing, and revising. Xiaoli Dong contributed in conceptualization, modifying, and revising. Ye Zhang contributed in conceptualization and reviewing. Renjie Chen contributed in conceptualization and reviewing. Xinbo Zhang contributed in conceptualization and reviewing. Yonggang Wang contributed in conceptualization and reviewing. All the authors read and approved the final version of the manuscript.

References

- [1] Chen C, Feng J, Li J, et al. Functional fiber materials to smart fiber devices. *Chem Rev* 2023;123:613–62.
- [2] Li JX, Liu YX, Yuan L, et al. A tissue-like neurotransmitter sensor for the brain and gut. *Nature* 2022;606:94–101.
- [3] Shi X, Zuo Y, Zhai P, et al. Large-area display textiles integrated with functional systems. *Nature* 2021;591:240–5.
- [4] Liao M, Wang C, Hong Y, et al. Industrial scale production of fibre batteries by a solution-extrusion method. *Nat Nanotechnol.* 2022;17:372–7.
- [5] He JQ, Lu CH, Jiang HB et al. Scalable production of high-performing woven lithium-ion fibre batteries. *Nature* 2021;597:57–63.
- [6] Wang S, Ouyang Z, Geng S, et al. A dynamically stable self-healable wire based on mechanical-electrical coupling. *Natl Sci Rev* 2024;11:nwae006.
- [7] Zhang A, Zhou L, Liang Q, et al. All-in-one multifunctional and stretchable electrochemical fiber enables health-monitoring textile with trace sweat. *Sci China Mater* 2023;67:251–60.
- [8] Lu C, Jiang H, Cheng X, et al. High-performance fibre battery with polymer gel electrolyte. *Nature* 2024;629:86–91.
- [9] Zhu YH, Yang XY, Liu T, et al. Flexible 1D batteries: Recent progress and prospects. *Adv Mater* 2020;32:1901961.
- [10] Mauger A, Julien CM, Goodenough JB, et al. Tribute to Michel Armand: From rocking chair–Li-ion to solid-state lithium batteries. *J Electrochem Soc* 2019;167:070507.
- [11] Ye L, Hong Y, Liao M et al. Recent advances in flexible fiber-shaped metal-air batteries. *Energy Storage Mater* 2020;28:364–74.
- [12] Xiang F, Cheng F, Sun Y, et al. Recent advances in flexible batteries: From materials to applications. *Nano Res* 2023;16:4821–54.
- [13] Zhu S, Sheng J, Chen Y, et al. Carbon nanotubes for flexible batteries: Recent progress and future

perspective. *Natl Sci Rev* 2021;8:nwaa261.

[14] Hu LB, Wu H, Mantia FL, et al. Thin, flexible secondary Li-ion paper batteries. *ACS Nano* 2010;4:5843–8.

[15] Yang Y, Jeong S, Hu LB, et al. Transparent lithium-ion batteries. *Proc Natl Acad Sci USA* 2011;108:13013–8.

[16] Wagner S, Lacour SP, Jones J, et al. Electronic skin: Architecture and components. *Phys E Low Dimens Syst Nanostruct* 2004;25:326–34.

[17] Qian J, Chen QY, Hong M, et al. Toward stretchable batteries: 3D-printed deformable electrodes and separator enabled by nanocellulose. *Mater Today* 2022;54:18–26.

[18] Li N, Chen HS, Yang SQ, et al. Bidirectional planar flexible snake-origami batteries. *Adv Sci* 2021;8:2101372.

[19] Liu GZ, Zhang XY, Lu B, et al. Crocodile skin inspired rigid-supple integrated flexible lithium ion batteries with high energy density and bidirectional deformability. *Energy Storage Mater* 2022;47:149–57.

[20] Kong L, Tang C, Peng HJ, et al. Advanced energy materials for flexible batteries in energy storage: A review. *SmartMat* 2020;1:e1007.

[21] Zhou Y, Wang CH, Lu W, et al. Recent advances in fiber-shaped supercapacitors and lithium-ion batteries. *Adv Mater* 2020;32:1902779.

[22] Yadav A, De B, Singh SK, et al. Facile development strategy of a single carbon-fiber-based all-solid-state flexible lithium-ion battery for wearable electronics. *ACS Appl Mater Interfaces* 2019;11:7974–80.

[23] Ren J, Zhang Y, Bai WY, et al. Elastic and wearable wire-shaped lithium-ion battery with high electrochemical performance. *Angew Chem Int Edit* 2014;126:7998–8003.

[24] Wang K, Zhang XH, Han JW, et al. High-performance cable-type flexible rechargeable Zn battery based on MnO₂@CNT fiber microelectrode. *ACS Appl Mater Interfaces* 2018;10:24573–82.

[25] Fang X, Weng W, Ren J, et al. A cable-shaped lithium sulfur battery. *Adv Mater* 2016;28:491–6.

[26] Sun H, You X, Jiang YS, et al. Self-healable electrically conducting wires for wearable microelectronics. *Angew Chem Int Edit* 2014;53:9680–5.

[27] Weng W, Sun Q, Zhang Y, et al. Winding aligned carbon nanotube composite yarns into coaxial fiber full batteries with high performances. *Nano Lett* 2014;14:3432–8.

[28] Kwon YH, Woo SW, Jung HR, et al. Cable-type flexible lithium ion battery based on hollow multi-helix electrodes. *Adv Mater* 2012;24:5192–7.

[29] Koo M, Park KI, Lee SH, et al. Bendable inorganic thin-film battery for fully flexible electronic systems.

Nano Lett 2012;12:4810–6.

[30] Xu S, Zhang YH, Cho J, et al. Stretchable batteries with self-similar serpentine interconnects and integrated wireless recharging systems. *Nat Commun* 2013;4:1543.

[31] Zeng K, Shi X, Tang C, et al. Design, fabrication and assembly considerations for electronic systems made of fibre devices. *Nat Rev Mater* 2023;8:552–61.

[32] Wang J, Wang Z, Ni J, et al. Electrospun materials for batteries moving beyond lithium-ion technologies. *Electrochem Energy Rev* 2021;5:211–41.

[33] Praveen S, Sim G, Ho C, et al. 3D-printed twisted yarn-type Li-ion battery towards smart fabrics. *Energy Storage Mater* 2021;41:748–57.

[34] Zhang K, Shi X, Jiang H, et al. Design and fabrication of wearable electronic textiles using twisted fiber-based threads. *Nat Protoc* 2024;19:1557–89.

[35] Zeng L, Chen S, Liu M, et al. Integrated paper-based flexible Li-ion batteries made by a rod coating method. *ACS Appl Mater Interfaces* 2019;11:46776–82.

[36] Chen X, Huang H, Pan L, et al. Fully integrated design of a stretchable solid-state lithium-ion full battery. *Adv Mater* 2019;31:1904648.

[37] Zhou J, Dong H, Chen Y, et al. Carbon-coated TiNb_2O_7 nanosheet arrays as self-supported high mass-loading anodes for flexible Li-ion batteries. *Chem Commun* 2021;57:1822–5.

[38] Lin X, Xue D, Zhao L, et al. In-situ growth of 1T/2H-MoS₂ on carbon fiber cloth and the modification of SnS₂ nanoparticles: A three-dimensional heterostructure for high-performance flexible lithium-ion batteries. *Chem Eng J* 2019;356:483–91.

[39] Zhang F, Teng X, Shi W, et al. SnO₂ nanoflower arrays on an amorphous buffer layer as binder-free electrodes for flexible lithium-ion batteries. *Appl Surface Sci* 2020;527:146910.

[40] Kim H, Kim D, Kim S, et al. Freestanding conversion-type anode via one-pot formation for flexible Li-ion battery. *Chem Eng J* 2022;427:130937.

[41] Chaturvedi P, Kanagaraj A, Choi D. LiCrTiO₄-MWCNT self-standing electrodes as high performance anode for flexible Li-ion batteries. *Mater Lett* 2021;304:130665.

[42] Bubulinca C, Sapurina I, Kazantseva N, et al. Fabrication of a flexible binder-free lithium manganese oxide cathode for secondary Li-ion batteries. *J Phys Chem Solids* 2020;137:109222.

[43] Li X, Wang X, Li J, et al. High-performance, flexible, binder-free silicon-carbon anode for lithium storage applications. *Electrochem Commun* 2022;137:107257.

[44] Praveen S, Sim G, Shaji N, et al. 3D-printed self-standing electrodes for flexible Li-ion batteries. *Appl Mater Today* 2022;26:100980.

- [45] Bao Y, Liu Y, Kuang Y, et al. 3D-printed highly deformable electrodes for flexible lithium ion batteries. *Energy Storage Mater* 2020;33:55–61.
- [46] Bao Y, Hong G, Chen Y, et al. Customized kirigami electrodes for flexible and deformable lithium-ion batteries. *ACS Appl Mater Interfaces* 2020;12:780–8.
- [47] Xu R, Zverev A, Hung A, et al. Kirigami-inspired, highly stretchable micro-supercapacitor patches fabricated by laser conversion and cutting. *Microsyst Nanoeng* 2018;4:36–45.
- [48] Qu S, Liu B, Wu J, et al. Kirigami-inspired flexible and stretchable zinc-air battery based on metal-coated sponge electrodes. *ACS Appl Mater Interfaces* 2020;12:54833–41.
- [49] Dai C, Sun G, Hu L, et al. Recent progress in graphene-based electrodes for flexible batteries. *InfoMat* 2019;2:509–26.
- [50] Guo J, Wang Y, Zhang H, et al. 3D-metal-embroidered electrodes: Dreaming for next generation flexible and personalizable energy storage devices. *Sci Bull* 2020;65:917–25.
- [51] Liu L, Zhang D, Yang T, et al. Flexible ion-conducting membranes with 3D continuous nanohybrid networks for high-performance solid-state metallic lithium batteries. *J Energy Chem* 2022;75:360–8.
- [52] Zhao L, Qu Z. Advanced flexible electrode materials and structural designs for sodium ion batteries. *J Energy Chem* 2022;71:108–28.
- [53] Li S, Dong R, Li Y, et al. Advances in free-standing electrodes for sodium ion batteries. *Mater Today* 2024;72:207–34.
- [54] Shen X, Yu H, Ben L, et al. High energy density in ultra-thick and flexible electrodes enabled by designed conductive agent/binder composite. *J Energy Chem* 2024;90:133–43.
- [55] Zou J, Zhang J, Wang L, et al. An all-from-one strategy to flexible solid-state lithium-ion batteries with decreased interfacial resistance. *Sci Chin Mater* 2024;67:1445–54.
- [56] Yuan S, Huang X, Kong T, et al. Organic electrode materials for energy storage and conversion: Mechanism, characteristics, and applications. *Accounts Chem Res* 2024;57:1550–63.
- [57] Bao Y, Liu H, Zhao Z, et al. Toward flexible embodied energy: Scale-inspired overlapping lithium-ion batteries with high-energy-density and variable stiffness. *Adv Funct Mater* 2023;33:2301581.
- [58] Liu Y, Peng H. Knittable and washable aerogel fiber inspired by polar bear hair. *Sci China Mater* 2024;67:705–6.
- [59] Wu N, Shi YR, Lang SY, et al. Self-healable solid polymeric electrolytes for stable and flexible lithium metal batteries. *Angew Chem Int Edit* 2019;58:18146–9.
- [60] Zhang Y, Yu L, Zhang XD, et al. A smart risk-responding polymer membrane for safer batteries. *Sci Adv* 2023;9:eade5802.

- [61] Tian YF, Tan SJ, Yang C, et al. Tailoring chemical composition of solid electrolyte interphase by selective dissolution for long-life micron-sized silicon anode. *Nat Commun* 2023;14:7247.
- [62] Goikolea E, Palomares V, Wang S, et al. Na-ion batteries-Approaching old and new challenges. *Adv Energy Mater* 2020;10:2002055.
- [63] Wang D, Cao L, Luo D, et al. Chain mail heterostructured hydrangea-like binary metal sulfides for high efficiency sodium ion battery. *Nano Energy* 2021;87:106185.
- [64] Zhao R, Sun N, Xu B, et al. Recent advances in heterostructured carbon materials as anodes for sodium-ion batteries. *Small Struct* 2021;2:2100132.
- [65] Kim EJ, Kumar PR, Gossage ZT, et al. Active material and interphase structures governing performance in sodium and potassium ion batteries. *Chem Sci* 2022;13:6121–58.
- [66] Wang J, Yue X, Xie Z, et al. MOFs-derived transition metal sulfide composites for advanced sodium ion batteries. *Energy Storage Mater* 2021;41:404–26.
- [67] Zhao C, Lu Y, Chen L, Hu Y. Flexible Na batteries. *InfoMat* 2020;2:126–38.
- [68] Wang HG, Li W, Liu DP, et al. Flexible electrodes for sodium-ion batteries: Recent progress and perspectives. *Adv Mater* 2017;29:1703012.
- [69] Zhu Y H, Yuan S, Bao D, et al. Decorating waste cloth via industrial wastewater for tube-type flexible and wearable sodium-ion batteries. *Adv Mater* 2017;29:1603719.
- [70] Hwang JY, Myung ST, Sun YK. Sodium-ion batteries: Present and future. *Chem Soc Rev* 2017;46:3529–614.
- [71] Zhang X, Zhou J, Liu C, et al. A universal strategy to prepare porous graphene films: Binder-free anodes for high-rate lithium-ion and sodium-ion batteries. *J Mater Chem A* 2016;4:8837–43.
- [72] Wang J, Wang Z, Ni J, et al. Electrospinning for flexible sodium-ion batteries. *Energy Storage Mater* 2022;45:704–19.
- [73] Balogun MS, Luo Y, Lyu F, et al. Carbon quantum dot surface-engineered VO₂ interwoven nanowires: A flexible cathode material for lithium and sodium ion batteries. *ACS Appl Mater Interfaces* 2016;8:9733–44.
- [74] Yang D, Liao XZ, Shen J, et al. A flexible and binder-free reduced graphene oxide/Na_{2/3}[Ni_{1/3}Mn_{2/3}]O₂ composite electrode for high-performance sodium ion batteries. *J Mater Chem A* 2014;2:6723–6.
- [75] Yu T, Lin B, Li Q, et al. First exploration of freestanding and flexible Na_{2+2x}Fe_{2-x}(SO₄)₃@porous carbon nanofiber hybrid films with superior sodium intercalation for sodium ion batteries. *Phys Chem Chem Phys* 2016;18:26933–41.

- [76] Sun Y, Liang X, Xiang H, et al. Free-standing vanadium pentoxide nanoribbon film as a high-performance cathode for rechargeable sodium batteries. *Chin Chem Lett* 2017;28:2251–53.
- [77] Wan P, Xie H, Zhang N, et al. Stepwise hollow Prussian blue nanoframes/carbon nanotubes composite film as ultrahigh rate sodium ion cathode. *Adv Funct Mater* 2020;30:2002624.
- [78] Nie P, Shen L, Pang G, et al. Flexible metal–organic frameworks as superior cathodes for rechargeable sodium-ion batteries. *J Mater Chem A* 2015;3:16590–7.
- [79] Sun T, Li ZJ, Wang HG, et al. A bio-degradable polydopamine-derived electrode material for high-capacity and long-life lithium-ion and sodium-ion batteries. *Angew Chem Int Edit* 2016;55:10662–6.
- [80] Zhou M, Li W, Gu T, et al. A sulfonated polyaniline with high density and high rate Na-storage performances as a flexible organic cathode for sodium ion batteries. *Chem Commun* 2015;51:14354–6.
- [81] Liu T, Kim KC, Lee B, et al. Self-polymerized dopamine as an organic cathode for Li- and Na-ion batteries. *Energy Environ Sci* 2017;10:205–15.
- [82] Zhang W, Zhang F, Ming F, Alshareef HN. Sodium-ion battery anodes: Status and future trends. *EnergyChem* 2019;1:100012.
- [83] Gu X, Wang S, Wang L, et al. TiO₂ nanotubes array on carbon cloth as a flexibility anode for sodium-ion batteries. *J Nanosci Nanotechnol* 2019;19:226.
- [84] Xie X, Kretschmer K, Zhang J, et al. Sn@CNT nanopillars grown perpendicularly on carbon paper: A novel free-standing anode for sodium ion batteries. *Nano Energy* 2015;13:208–17.
- [85] Liang L, Xu Y, Wang C, et al. Large-scale highly ordered Sb nanorod array anodes with high capacity and rate capability for sodium-ion batteries. *Energy Environ Sci* 2015;8:2954–62.
- [86] Sun N, Guan Y, Liu Y, et al. Facile synthesis of free-standing, flexible hard carbon anode for high-performance sodium ion batteries using graphene as a multi-functional binder. *Carbon* 2018;137:475–83.
- [87] Sun N, Zhu Q, Babak A, et al. MXene-bonded flexible hard carbon film as anode for stable Na/K-ion storage. *Adv Funct Mater* 2019;29:1906282.
- [88] Beda A, Villevieille C, Taberna PL, et al. Self-supported binder-free hard carbon electrodes for sodium-ion batteries: Insights into their sodium storage mechanisms. *J Mater Chem A* 2020;8:5558–71.
- [89] Wang S, Xia L, Yu L, et al. Free-standing nitrogen-doped carbon nanofiber films: Integrated electrodes for sodium-ion batteries with ultralong cycle life and superior rate capability. *Adv Energy Mater* 2016;6:1502217.
- [90] Zhang X, Zhou J, Liu C, et al. A universal strategy to prepare porous graphene films: Binder-free anodes for high-rate lithium-ion and sodium-ion batteries. *J Mater Chem A* 2016;4:8837–43.
- [91] Li Z, Shen W, Wang C, et al. Ultra-long Na₂Ti₃O₇ nanowires@carbon cloth as a binder-free flexible

- electrode with a large capacity and long lifetime for sodium-ion batteries. *J Mater Chem A* 2016;4:17111–20.
- [92] Xie D, Xia X, Zhong Y, et al. Exploring advanced sandwiched arrays by vertical graphene and N-doped carbon for enhanced sodium storage. *Adv Energy Mater* 2017;7:1601804.
- [93] Xie X, Kretschmer K, Zhang J, et al. Sn@CNT nanopillars grown perpendicularly on carbon paper: A novel free-standing anode for sodium ion batteries. *Nano Energy* 2015;13:208–17.
- [94] Liu Y, Zhang A, Shen C, et al. Red phosphorus nanodots on reduced graphene oxide as a flexible and ultra-fast anode for sodium-ion batteries. *ACS Nano* 2017;11:5530–7.
- [95] Wu X, Ma J, Ma Q, et al. A spray drying approach for the synthesis of a $\text{Na}_2\text{C}_6\text{H}_2\text{O}_4/\text{CNT}$ nanocomposite anode for sodium-ion batteries. *J Mater Chem A* 2015;3:13193–7.
- [96] Gao H, Zhou W, Park K, Goodenough JB. A sodium-ion battery with a low-cost cross-linked gel-polymer electrolyte. *Adv Energy Mater* 2016;6:1600467.
- [97] Zhang Y, Wu F, Huang Y, et al. A novel gel polymer electrolyte doped with MXene enables dendrite-free cycling for high-performance sodium metal batteries. *J Mater Chem A* 2022;10:11553–61.
- [98] Kumar D, Hashmi SA. Ion transport and ion-filler-polymer interaction in poly(methyl methacrylate)-based, sodium ion conducting, gel polymer electrolytes dispersed with silica. *J Power Sources* 2010;195:5101–8.
- [99] Shen L, Deng S, Jiang R, et al. Flexible composite solid electrolyte with 80 wt% $\text{Na}_{3.4}\text{Zr}_{1.9}\text{Zn}_{0.1}\text{Si}_{2.2}\text{P}_{0.8}\text{O}_{12}$ for solid-state sodium batteries. *Energy Storage Mater* 2022;46:175–81.
- [100] Lin X, Zhao Y, Wang C, et al. A dual anion chemistry-based superionic glass enabling long-cycling all-solid-state sodium-ion batteries. *Angew Chem Int Edit* 2024;63:e202314181.
- [101] Guo Z, Zhao Y, Ding Y, et al. Multi-functional flexible aqueous sodium-ion batteries with high safety. *Chem* 2017;3:348–62.
- [102] Liu T, Du X, Wu H, et al. A Bio-inspired methylation approach to salt-concentrated hydrogel electrolytes for long-life rechargeable batteries. *Angew Chem Int Edit* 2023;62:e202311589.
- [103] Zhu YH, Yuan S, Bao D, et al. Decorating waste cloth via industrial wastewater for tube-type flexible and wearable sodium-ion batteries. *Adv Mater* 2017;29:1603719.
- [104] Zhang W, Liu YT, Chen CJ, et al. Flexible and binder-free electrodes of Sb/rGO and $\text{Na}_3\text{V}_2(\text{PO}_4)_3/\text{rGO}$ nanocomposites for sodium-ion batteries. *Small* 2015;11:3822–9.
- [105] Lu Q, Wang X, Cao J, et al. Freestanding carbon fiber cloth/sulfur composites for flexible room-temperature sodium-sulfur batteries. *Energy Storage Mater* 2017;8:77–84.
- [106] Ma J, Zheng S, Chi L, et al. 3D printing flexible sodium-ion microbatteries with ultrahigh areal capacity and robust rate capability. *Adv Mater* 2022;34:2205569.

- [107] Yu B, Ji Y, Hu X, et al. Heterostructured Cu₂S@ZnS/C composite with fast interfacial reaction kinetics for high-performance 3D-printed sodium-ion batteries. *Chem Eng J* 2022;430:132993.
- [108] Dong HB, Li JW, Guo J, et al. Insights on flexible zinc-ion batteries from lab research to commercialization. *Adv Mater* 2021;33:2007548.
- [109] Xiao X, Zheng ZY, Zhong XW, et al. Rational design of flexible Zn-based batteries for wearable electronic devices. *ACS Nano* 2023;17:1764–802.
- [110] Zhu S, Wang Q, Ni J. Aqueous transition-metal ion batteries: Materials and electrochemistry. *EnergyChem* 2023;5:100097.
- [111] Zhu J, Hu W, Ni J, et al. High areal energy zinc-ion micro-batteries enabled by 3D printing. *J Mater Sci Technol* 2024;196:183–9.
- [112] Yi Z, Chen G, Hou F, et al. Strategies for the stabilization of Zn metal anodes for Zn-ion batteries. *Adv Energy Mater* 2021;11:2003065.
- [113] Xu J, Li H, Jin Y, et al. Understanding the electrical mechanisms in aqueous zinc metal batteries: From electrostatic interactions to electric field regulation. *Adv Mater* 2024;36:02309726.
- [114] Wang Y, Li Q, Hong H, et al. Lean-water hydrogel electrolyte for zinc ion batteries. *Nat Commun* 2023;14:3890.
- [115] Shi Y, Wang R, Bi S, et al. An anti-freezing hydrogel electrolyte for flexible zinc-ion batteries operating at –70 °C. *Adv Funct Mater* 2023;33:202214546.
- [116] Liu Q, Yu Z, Zhuang Q, et al. Anti-fatigue hydrogel electrolyte for all-flexible Zn-ion batteries. *Adv Mater* 2023;35:202300498.
- [117] Zhu Y, Fan J, Zhang S, et al. Long-life flexible mild Ag-Zn fibrous battery with bifunctional gel electrolyte. *Chem Eng J* 2024;480:148334.
- [118] Li C, Wang W, Sun X, et al. Ultra-durable and flexible fibrous mild quasi-solid-state Ag-Zn batteries with Na₂SO₄ electrolyte additive. *J Mater Chem A* 2022;10:24708–16.
- [119] Gao TT, Yan GY, Yang X, et al. Wet spinning of fiber-shaped flexible Zn-ion batteries toward wearable energy storage. *J Energy Chem* 2022;71:192–200.
- [120] Pu J, Cao QH, Gao Y, et al. Liquid metal-based stable and stretchable Zn-ion battery for electronic textiles. *Adv Mater* 2024;36:202305812.
- [121] Li M, Li Z, Ye X, et al. Tendril-inspired 900% ultrastretching fiber-based Zn-ion batteries for wearable energy textiles. *ACS Appl Mater Interfaces* 2021;13:17110–7.
- [122] Javed MS, Lei H, Wang Z, et al. 2D V₂O₅ nanosheets as a binder-free high-energy cathode for ultrafast aqueous and flexible Zn-ion batteries. *Nano Energy* 2020;70:104573.

- [123] Chen T, Wang YA, Yang Y, et al. Heterometallic seed-mediated zinc deposition on inkjet printed silver nanoparticles toward foldable and heat-resistant zinc batteries. *Adv Funct Mater* 2021;31:2101607.
- [124] Wang JH, Chen LF, Dong WX, et al. Three-dimensional zinc-seeded carbon nanofiber architectures as lightweight and flexible hosts for a highly reversible zinc metal anode. *ACS Nano* 2023;17:19087–97.
- [125] Liu Q, Ou X, Niu Y, et al. Flexible Zn-ion electrochromic batteries with multiple-color variations. *Angew Chem Int Edit* 2024;63:e202317944.
- [126] Huang S, Hou L, Li T, et al. Antifreezing hydrogel electrolyte with ternary hydrogen bonding for high-performance zinc-ion batteries. *Adv Mater* 2022;34:202110140.
- [127] Long J, Han T, Lin X, et al. An integrated flexible self-healing Zn-ion battery using dendrite-suppressible hydrogel electrolyte and free-standing electrodes for wearable electronics. *Nano Res* 2023;16:11000–11.
- [128] Yin L, Scharf J, Ma J, et al. High performance printed AgO-Zn rechargeable battery for flexible electronics. *Joule* 2021;5:228–48.
- [129] Liu H, Li J, Wei D, et al. Biomimetic honeycomb Zn anode enabled multi-field regulation toward highly stable flexible Zn-ion batteries. *Adv Funct Mater* 2023;33:2300419.
- [130] Zeng L, He J, Yang C, et al. Direct 3D printing of stress-released Zn powder anodes toward flexible dendrite-free Zn batteries. *Energy Storage Mater* 2023;54:469–77.
- [131] Zhao X, Gao Y, Cao Q, et al. A high-capacity gradient Zn powder anode for flexible Zn-ion batteries. *Adv Energy Mater* 2023;13:202301741.
- [132] Yu H, Liu D, Feng X, et al. Mini review: Recent advances on flexible rechargeable Li-air batteries. *Energy Fuels* 2021;35:4751–61.
- [133] Cao X, Wei C, Zheng X, et al. Ru clusters anchored on Magnéli phase Ti_4O_7 nanofibers enables flexible and highly efficient Li- O_2 batteries. *Energy Storage Mater* 2022;50:355–64.
- [134] Zhang K, Wu F, Wang X, et al. 8.5 μm -thick flexible-rigid hybrid solid-electrolyte/lithium integration for air-stable and interface-compatible all-solid-state lithium metal batteries. *Adv Energy Mater* 2022;12:2200368.
- [135] Xia J, Yin S, Cui K, et al. Self-catalyzed growth of Co_4N and N-doped carbon nanotubes toward bifunctional cathode for highly safe and flexible Li-air batteries. *ACS Nano* 2024;18:10902–11.
- [136] Li J, He X, Yuan W, et al. A highly stable long-cycle lithium-oxygen battery based on flexible PVDF-HFP@LTP solid-state electrolyte. *ACS Appl Energy Mater* 2024;7:3484–96.
- [137] Liu Y, Yao M, Zhang L, et al. Large-scale fabrication of reduced graphene oxide-sulfur composite films for flexible lithium-sulfur batteries. *J Energy Chem* 2019;38:199–206.

- [138] Gao Y, Guo Q, Zhang Q, et al. Fibrous materials for flexible Li-S battery. *Adv Energy Mater* 2020;11:2002580.
- [139] Zhao CX, Li XY, Zhao M, et al. Semi-immobilized molecular electrocatalysts for high-performance lithium-sulfur batteries. *J Am Chem Soc* 2021;143:19865–72.
- [140] Zhang Y, Zhang P, Zhang S, et al. A flexible metallic TiC nanofiber/vertical graphene 1D/2D heterostructured as active electrocatalyst for advanced Li-S batteries. *InfoMat* 2021;3:790–803.
- [141] Sheng J, Zhang Q, Sun C, et al. Crosslinked nanofiber-reinforced solid-state electrolytes with polysulfide fixation effect towards high safety flexible lithium-sulfur batteries. *Adv Funct Mater* 2022;32:2203272.
- [142] Zhang T, Shao W, Liu S, et al. A flexible design strategy to modify $\text{Ti}_3\text{C}_2\text{T}_x$ MXene surface terminations via nucleophilic substitution for long-life Li-S batteries. *J Energy Chem* 2022;74:349–58.
- [143] Hu JK, Yuan H, Yang SJ, et al. Dry electrode technology for scalable and flexible high-energy sulfur cathodes in all-solid-state lithium-sulfur batteries. *J Energy Chem* 2022;71:612–8.
- [144] Xia J, Chen W, Yang Y, et al. In-situ growth of ultrathin sulfur microcrystal on MXene-based 3D matrice for flexible lithium-sulfur batteries. *EcoMat* 2022;4:e12183.
- [145] Yao G, Li Z, Zhang Y, et al. Highly flexible carbon film implanted with single-atomic Zn-N₂ moiety for long-life sodium-sulfur batteries. *Adv Funct Mater* 2023;34:2214353.
- [146] Lu K, Li B, Zhan X, et al. Elastic Na_xMoS_2 -carbon-base triple interface direct robust solid-solid interface for all-solid-state Na-S batteries. *Nano Lett* 2020;20:6837–44.
- [147] Liu H, Pei W, Lai WH, et al. Electrocatalyzing S cathodes via multisulfiphilic sites for superior room-temperature sodium-sulfur batteries. *ACS Nano* 2020;14:7259–68.
- [148] Kang JH, Lee J, Jung JW, et al. Lithium-air batteries: Air-breathing challenges and perspective. *ACS Nano* 2020;14:14549–78.
- [149] Wang Y, Lu YC. Nonaqueous lithium-oxygen batteries: Reaction mechanism and critical open questions. *Energy Storage Mater* 2020;28:235–46.
- [150] Zheng Z, Wu C, Gu Q, et al. Research progress and future perspectives on rechargeable Na-O₂ and Na-CO₂ batteries. *Energy Environ Mater* 2021;4:158–77.
- [151] Hartmann P, Bender CL, Vracar M, et al. A rechargeable room-temperature sodium superoxide (NaO₂) battery. *Nat Mater* 2013;12:228–32.
- [152] Huang B, Zhang W, Chen J, et al. Review-research progress and prospects of Li-air battery in wearable devices. *J Electrochem Soc* 2023;170:020506.
- [153] Zhu X, Wu Y, Wang Z, et al. Hierarchical architecture: A novel, facile and cost-efficient strategy to

boost electrochemical performance of Li-O₂ battery cathodes. *Chem Eng J* 2022;450:138462.

[154] Yang XY, Xu JJ, Chang ZW, et al. Blood-capillary-inspired, free-standing, flexible, and low-cost super-hydrophobic N-CNTs@SS cathodes for high-capacity, high-rate, and stable Li-air batteries. *Adv Energy Mater* 2018;8:1702242.

[155] Jung JW, Nam JS, Klyukin K, et al. Straightforward strategy toward a shape-deformable carbon-free cathode for flexible Li-air batteries in ambient air. *Nano Energy* 2021;83:105821.

[156] Cao X, Wei C, Zheng X, et al. Ru clusters anchored on Magnéli phase Ti₄O₇ nanofibers enables flexible and highly efficient Li-O₂ batteries. *Energy Storage Mater* 2022;50:355–64.

[157] Guo L, Zhang G, Yang R, et al. Pd cluster decorated free standing flexible cathode for high performance Li-oxygen batteries. *Nano Res* 2023;17:2678–86.

[158] Zhang Q, Lei X, Lv Y, et al. Liquid metal-based cathode for flexible ambient Li-air batteries and its regeneration by water. *Appl Surf Sci* 2023;607:155074.

[159] Liu X, Lei X, Wang YG, et al. Prevention of Na corrosion and dendrite growth for long-life flexible Na-air batteries. *ACS Cent Sci* 2021;7:335–44.

[160] Fu Y, Lei X, Yin H, et al. Rational reconfiguration of a gradient redox mediator with in-situ fabricated gel electrolyte for Li-air batteries. *Chem Eng J* 2021;416:129016.

[161] Wang J, Ni Y, Liu J, et al. Room-temperature flexible quasi-solid-state rechargeable Na-O₂ batteries. *ACS Cent Sci* 2020;6:1955–63.

[162] Shu C, Long J, Dou SX, et al. Component-interaction reinforced quasi-solid electrolyte with multifunctionality for flexible Li-O₂ battery with superior safety under extreme conditions. *Small* 2019;15:1804701.

[163] Chi X, Li M, Di J, et al. A highly stable and flexible zeolite electrolyte solid-state Li-air battery. *Nature* 2021;592:551–7.

[164] Liu T, Feng XL, Jin X, et al. Protecting the lithium metal anode for a safe flexible lithium-air battery in ambient air. *Angew Chem Int Edit* 2019;131:18408–13.

[165] Ye L, Cheng X, Liao M, et al. Deformation-tolerant metal anodes for flexible sodium-air fiber batteries. *eScience* 2022;2:606–14.

[166] Zou X, Liao K, Wang D, et al. Water-proof, electrolyte-nonvolatile, and flexible Li-air batteries via O₂-permeable silica-aerogel-reinforced polydimethylsiloxane external membranes. *Energy Storage Mater* 2020;27:297–306.

[167] Liu T, Yu Y, Yang XY, et al. Lithium and stannum hybrid anodes for flexible wire-type lithium-oxygen batteries. *Small Struct* 2020;1:2000015.

- [168] Zhang Y, Wang L, Guo Z, et al. High-performance lithium-air battery with a coaxial-fiber architecture. *Angew Chem Int Edit* 2016;55:4487–91.
- [169] Jaradat A, Zhang C, Singh SK, et al. High performance air breathing flexible lithium-air battery. *Small* 2021;17:2102072.
- [170] Yang XY, Feng XL, Jin X, et al. An illumination-assisted flexible self-powered energy system based on a Li-O₂ battery. *Angew Chem Int Edit* 2019;58:16411–5.
- [171] Wei L, Su Y, Ma Y, et al. Photoluminescent WSe₂ nanofibers as freestanding cathode for solar-assisted Li-O₂ battery with ultrahigh capacity and transparent casing. *Chem Eng J* 2022;448:137591.
- [172] Zhou J, Cheng J, Wang B, et al. Flexible metal-gas batteries: A potential option for next-generation power accessories for wearable electronics. *Energy Environ Sci* 2020;13:1933–70.
- [173] Balamurugan J, Austeria PM, Kim JB, et al. Electrocatalysts for zinc-air batteries featuring single molybdenum atoms in a nitrogen-doped carbon framework. *Adv Mater* 2023;35:2302625.
- [174] Chen Y, Xu J, He P, et al. Metal-air batteries: Progress and perspective. *Sci Bull* 2022;67:2449–86.
- [175] Li L, Tsang YCA, Xiao D, et al. Phase-transition tailored nanoporous zinc metal electrodes for rechargeable alkaline zinc-nickel oxide hydroxide and zinc-air batteries. *Nat Commun* 2022;13:2870.
- [176] Wang Y, Cao Q, Guan C, et al. Recent advances on self-supported arrayed bifunctional oxygen electrocatalysts for flexible solid-state Zn-air batteries. *Small* 2020;16:2002902.
- [177] Liu JN, Zhao CX, Ren D, et al. Preconstructing asymmetric interface in air cathodes for high-performance rechargeable Zn-air batteries. *Adv Mater* 2022;34:2109407.
- [178] Bi X, Jiang Y, Chen R, et al. Rechargeable zinc-air versus lithium-air battery: From fundamental promises toward technological potentials. *Adv Energy Mater* 2024;14:2302388.
- [179] Luo X, Yang M, Song W, et al. Neutral Zn-air battery assembled with single-atom iridium catalysts for sensitive self-powered sensing system. *Adv Funct Mater*. 2021;31:2101193.
- [180] Sun W, Wang F, Zhang B, et al. A rechargeable zinc-air battery based on zinc peroxide chemistry. *Science* 2021;371:46–51.
- [181] Wu WF, Yan X, Zhan Y. Recent progress of electrolytes and electrocatalysts in neutral aqueous zinc-air batteries. *Chem Eng J* 2023;451:138608.
- [182] Zhang T, Wu N, Zhao Y, et al. Frontiers and structural engineering for building flexible zinc-air batteries. *Adv Sci* 2022;9:2103954.
- [183] Pei Z, Ding L, Wang C, et al. Make it stereoscopic: Interfacial design for full-temperature adaptive flexible zinc-air batteries. *Energy Environ Sci* 2021;14:4926–35.

- [184] Hui X, Zhang P, Li J, et al. In situ integrating highly ionic conductive LDH-array@PVA gel electrolyte and MXene/Zn anode for dendrite-free high-performance flexible Zn-air batteries. *Adv Energy Mater* 2022;12:2201393.
- [185] Fan X, Zhang R, Sui S, et al. Starch-based superabsorbent hydrogel with high electrolyte retention capability and synergistic interface engineering for long-lifespan flexible zinc-air batteries. *Angew Chem Int Edit* 2023;62:e202302640.
- [186] Dou H, Xu M, Zheng Y, et al. Bioinspired tough solid-state electrolyte for flexible ultralong-life zinc-air battery. *Adv Mater* 2022;34:2110585.
- [187] Qu S, Liu J, Han X, et al. Dynamic stretching-electroplating metal-coated textile for a flexible and stretchable zinc-air battery. *Carbon Energy* 2022;4:867–77.
- [188] Qu S, Liu B, Wu J, et al. Kirigami-Inspired flexible and stretchable zinc-air battery based on metal-coated sponge electrodes. *ACS Appl Mater Interfaces* 2020;12:54833–41.
- [189] Ma L, Chen S, Wang D, et al. Super-stretchable zinc-air batteries based on an alkaline-tolerant dual-network hydrogel electrolyte. *Adv Energy Mater* 2019;9:1803046.
- [190] Xu Q, Chen J, Loh JR, et al. Fiber-shaped batteries towards high performance and perspectives of corresponding integrated battery textiles. *Adv Energy Mater* 2024;14:2302536.
- [191] Ye L, Hong Y, Liao M, et al. Recent advances in flexible fiber-shaped metal-air batteries. *Energy Storage Mater* 2020;28:364–74.
- [192] Huang H, Huang A, Liu D, et al. Tailoring oxygen reduction reaction kinetics on perovskite oxides via oxygen vacancies for low-temperature and knittable zinc-air batteries. *Adv Mater* 2023;35:2303109.
- [193] Gu C, Xie XQ, Liang Y, et al. Small molecule-based supramolecular-polymer double-network hydrogel electrolytes for ultra-stretchable and waterproof Zn-air batteries working from –50 to 100 °C. *Energy Environ Sci* 2021;14:4451–62.
- [194] Chen S, Ma L, Wu S, et al. Uniform Virus-like Co-N-Cs electrocatalyst derived from prussian blue analog for stretchable fiber-shaped Zn-air batteries. *Adv Funct Mater* 2020;30:1908945.
- [195] Wang J, Zhang H, Yang L, et al. In situ implanting 3D carbon network reinforced zinc composite by powder metallurgy for highly reversible Zn-based battery anodes. *Angew Chem Int Edit* 2024;63:e202318149.
- [196] Chen H, Li L, Wang L, et al. High-performance neutral zinc-air batteries based on hybrid zinc/carbon nanotube fiber anodes. *Adv Mater Technol* 2023;8:2301217.
- [197] Liu R, Wang Z L, Fukuda K, et al. Flexible self-charging power sources. *Nat Rev Mater* 2022;7:870–86.

- [198] Sun Y, Li YZ, Yuan M. Requirements, challenges, and novel ideas for wearables on power supply and energy harvesting. *Nano Energy* 2023;115:108715.
- [199] Liu T, Zhao S, Wang Y, et al. In situ anchoring Co-N-C nanoparticles on Co₄N nanosheets toward ultrastable flexible self-supported bifunctional oxygen electrocatalyst enables recyclable Zn-air batteries over 10,000 cycles and fast charging. *Small* 2022;18:2105887.
- [200] He J, Cao L, Cui J, et al. Flexible energy storage devices to power the future. *Adv Mater* 2024;36:2306090.
- [201] Zhong X, Zheng Z, Xu J, et al. Flexible zinc-air batteries with ampere-hour capacities and wide-temperature adaptabilities. *Adv Mater* 2023;35:2209980.
- [202] Zhu YH, Yang XY, Liu T, et al. Flexible 1D batteries: Recent progress and prospects. *Adv Mater* 2020;32:1901961.
- [203] Zhang Y, Wu D, Huang F, et al. "Water-in-Salt" nonalkaline gel polymer electrolytes enable flexible zinc-air batteries with ultra-long operating time. *Adv Funct Mater* 2022;32:2203204.
- [204] Lee GH, Moon H, Kim H, et al. Multifunctional materials for implantable and wearable photonic healthcare devices. *Nat Rev Mater* 2020;5:149–65.
- [205] Li L, Li D, Wang Y, et al. Implantable zinc-oxygen battery for in situ electrical stimulation-promoted neural regeneration. *Adv Mater* 2023;35:2302997.
- [206] Xia D, Yang F, Zheng Y, et al. Research status of biodegradable metals designed for oral and maxillofacial applications: A review. *Bioact Mater* 2021;6:4186–208.
- [207] Liu F, Wang T, Liu X, et al. Challenges and recent progress on key materials for rechargeable magnesium batteries. *Adv Energy Mater* 2021;11:2000787.
- [208] Huang X, Liu Y, Park W, et al. Stretchable magnesium-air battery based on dual ions conducting hydrogel for intelligent biomedical applications. *InfoMat* 2023;5:e12388.
- [209] Ling W, Wang H, Chen Z, et al. Intrinsic structure modification of electrode materials for aqueous metal-ion and metal-air batteries. *Adv Funct Mater* 2021;31:2006855.
- [210] Cheng M, Yan R, Yang Z, et al. Polysulfide catalytic materials for fast-kinetic metal-sulfur batteries: Principles and active centers. *Adv Sci* 2022;9:2102217.
- [211] Cheng C, Li S, Xia Y, et al. Atomic Fe-N_x coupled open-mesoporous carbon nanofibers for efficient and bioadaptable oxygen electrode in Mg-air batteries. *Adv Mater* 2018;30:1802669.
- [212] Chen X, Zou Q, Le Q, et al. Influence of heat treatment on the discharge performance of Mg-Al and Mg-Zn alloys as anodes for the Mg-air battery. *Chem Eng J* 2022;433:133797.
- [213] Song Z, Wang J, Song Y, et al. In situ interfacial passivation in aqueous electrolyte for Mg-air batteries

with high anode utilization and specific capacity. *ChemSusChem* 2023;16:e202202207.

[214] Guo Z, Zhao S, Li T, et al. Recent advances in rechargeable magnesium-based batteries for high-efficiency energy storage. *Adv Energy Mater* 2020;10:1903591.

[215] Li L, Chen H, He E, et al. High-energy-density magnesium-air battery based on dual-layer gel electrolyte. *Angew Chem Int Edit* 2021;133:15445–50.

[216] Kim TY, An S, Kim Y, et al. Lubricant-infused polymeric interfaces: A stretchable and anti-fouling surface for implantable biomaterials. *Adv Funct Mater* 2023;34:2312740.

[217] Zhang D, Chen Q, Bi Y, et al. Bio-inspired poly-DL-serine materials resist the foreign-body response. *Nat Commun* 2021;12:5327.

[218] He E, Ren J, Wang L, et al. A mitochondrion-inspired magnesium-oxygen biobattery with high energy density in vivo. *Adv Mater* 2023;35:2304141.

[219] Liu Y, Huang X, Zhou J, et al. Bandage based energy generators activated by sweat in wireless skin electronics for continuous physiological monitoring. *Nano Energy* 2022;92:106755.

[220] Sheng H, Zhang X, Liang J, et al. Recent advances of energy solutions for implantable bioelectronics. *Adv Healthcare Mater* 2021;10:2100199.



Xiao Zhu is a Ph.D. candidate at the Department of Chemistry, Fudan University. He obtained his B.S. degree from Fudan University in 2022. His current research interest focuses on the design of novel solvents and electrolytes for lithium metal batteries and lithium-ion batteries.



Haoran Zhang is a Master Student at Changchun Institute of Applied Chemistry (CIAC), Chinese Academy of Sciences (CAS). His research interest focuses on the design and development of multifunctional catalysts and their application in Li-O₂ batteries.



Yongxin Huang is an associate professor at School of Materials, Beijing Institute of Technology. His main research directions include key materials and integration technology of sodium-ion batteries, new systems and mechanisms of high specific energy secondary batteries, advanced in-situ characterization technology and theoretical simulation technology.



Er He is a Ph.D. candidate for Materials Science and Engineering at the College of Engineering and Applied Science, Nanjing University. She received her B.S. degree in Materials at Donghua University in 2020. Her current research interest focuses on implantable energy devices and their biomedical applications.



Yun Shen is a Ph.D. candidate at Kunming University of Science and Technology. His research interest focuses on Li-metal-based batteries including lithium-sulfur batteries, Li-metal anodes.



Gang Huang received his Ph.D. degree in Applied Chemistry from University of Chinese Academy of Sciences in 2016. Now he works at CIAC, CAS as a professor, and his research focuses on the development and characterization of electrode materials for Li-metal and Zn-ion batteries.



Shouyi Yuan obtained his Ph.D. degree at Fudan University in 2021. He is now working at National and Local Joint Engineering Laboratory for Lithium-Ion Batteries and Materials Preparation Technology, Kunming University of Science and Technology. His research interest focuses on Li-metal-based batteries including lithium-sulfur batteries, lithium-oxygen batteries, Li-metal anodes, and aqueous batteries.



Xiaoli Dong received her Ph.D. degree in Physical Chemistry from Fudan University in 2017 and now she is an associate professor at the Department of Chemistry, Fudan University. Her research mainly focuses on the novel electrolytes and electrode materials for low temperature applications, including lithium-ion batteries, sodium-ion batteries, electrochemical capacitors, and new devices.



Ye Zhang is currently an associate professor at the College of Engineering and Applied Sciences, Nanjing University. She received her Ph.D. degree in Macromolecular Chemistry and Physics from Fudan University in 2018, and then joined Harvard Medical School as a postdoctoral research fellow. Her research interest includes functional polymer materials and soft polymer batteries.



Renjie Chen is a professor at the School of Materials Science and Engineering, Beijing Institute of Technology. He is mainly engaged in the research of new batteries and key energy materials. For the construction of new systems of high energy density batteries and the design and development of functional devices, he has carried out teaching and research work on new systems of multi-electron high specific energy batteries, new ionic liquids and functional composite electrolyte materials, special power sources and structural devices, smart batteries and information energy fusion cross-technology.

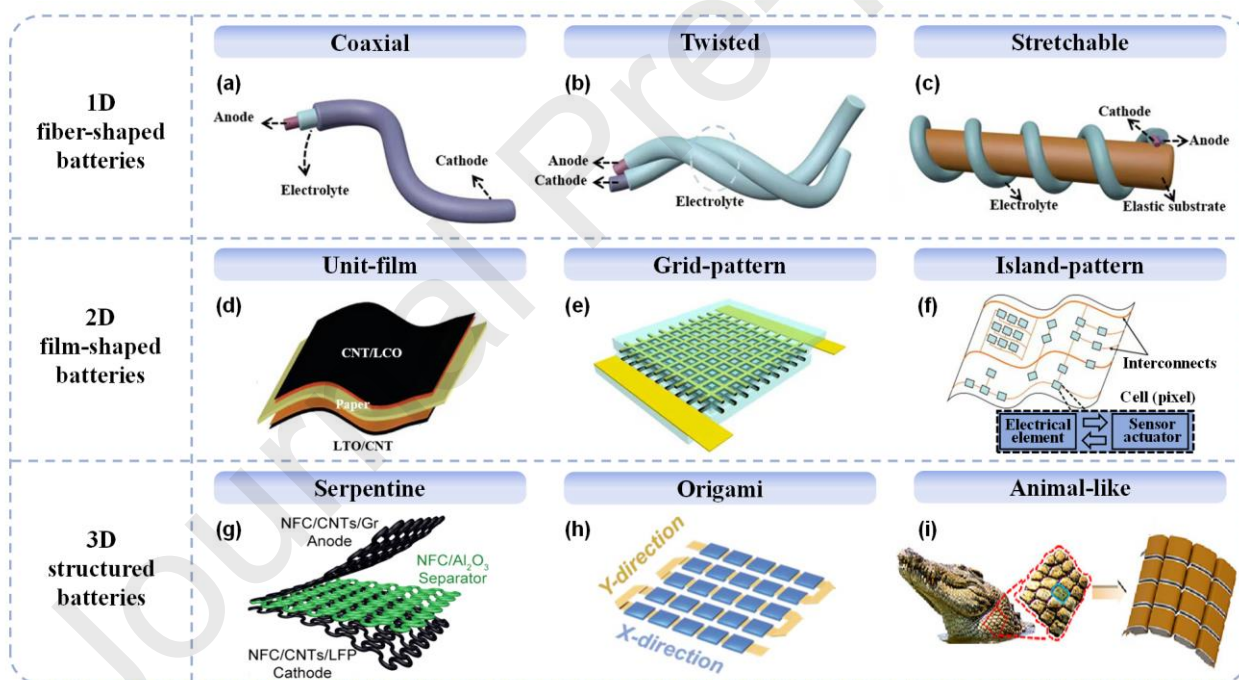
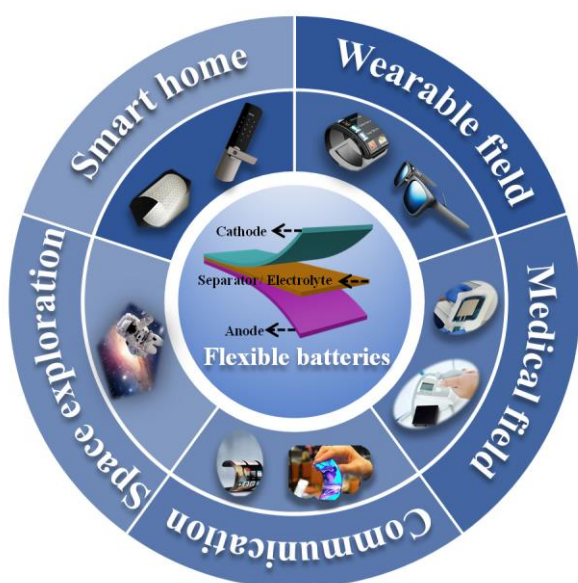


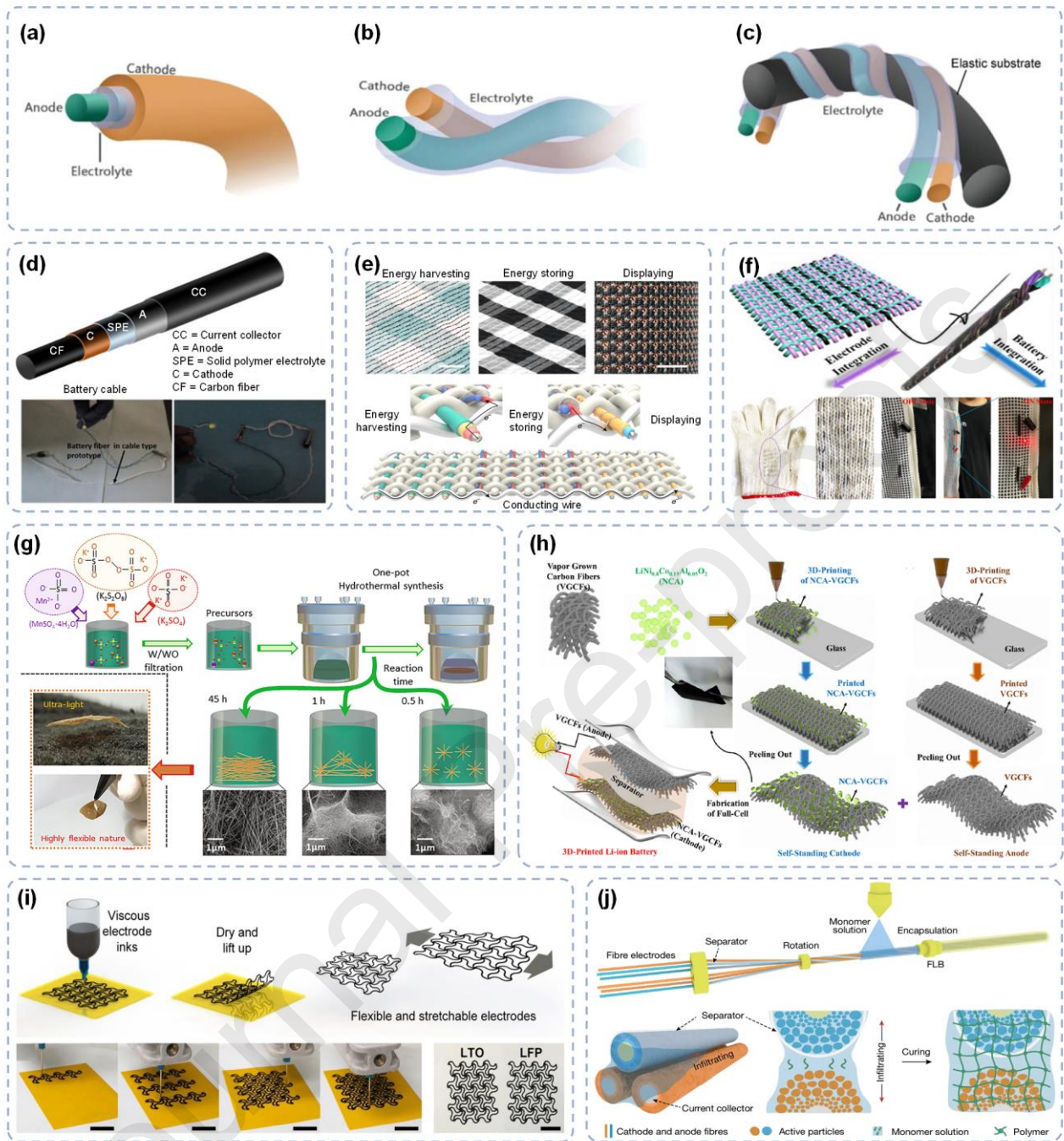
Xinbo Zhang joined CIAC, CAS as a professor in 2010. He received his Ph.D. degree in Inorganic Chemistry from CIAC. From 2005–2010, he worked as a JSPS and NEDO fellow at the National Institute of Advanced Industrial Science and Technology (Kansai Center), Japan. His interest mainly focuses on functional inorganic/organic materials for energy storage & conversion with fuel cells and batteries.



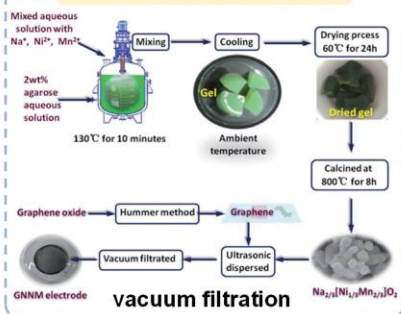
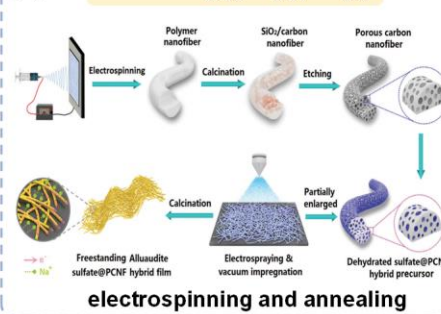
Yonggang Wang received his Ph.D. degree in Physical Chemistry from Fudan University in 2007. From 2007 to 2011, he worked as a postdoctoral research associate at AIST, Japan. He is currently a full professor at the Department of Chemistry, Fudan University. His research interest includes electrochemical functional materials and their application in lithium-ion batteries, lithium batteries, sodium-ion batteries, metal-air

batteries, supercapacitors, and water electrolysis.

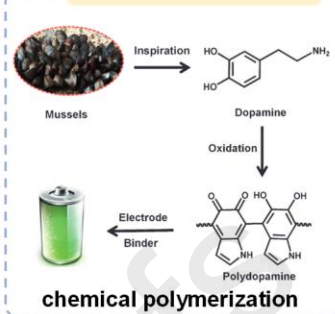




Cathodes for flexible SIBs

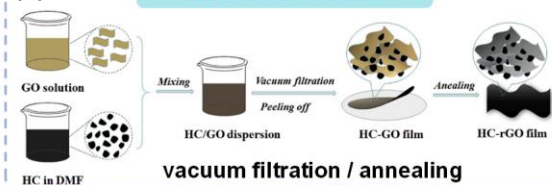
(a) $rGO/Na_{2/3}[Ni_{1/3}Mn_{2/3}]O_2$ (b) $CNFs/Na_{2+2x}Fe_{2-x}(SO_4)_3$ 

(c) PDA with catechol

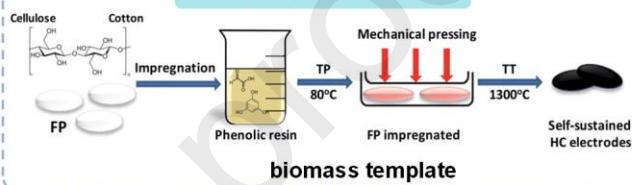


Anodes for flexible SIBs

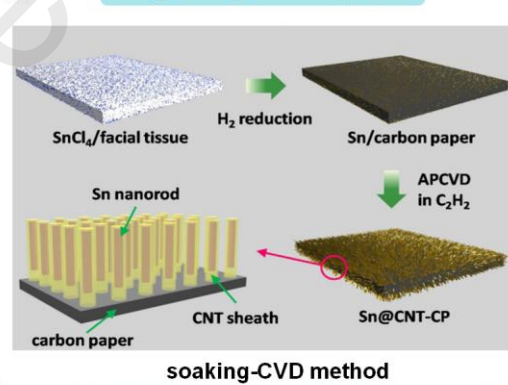
(d) rGO/hard carbon

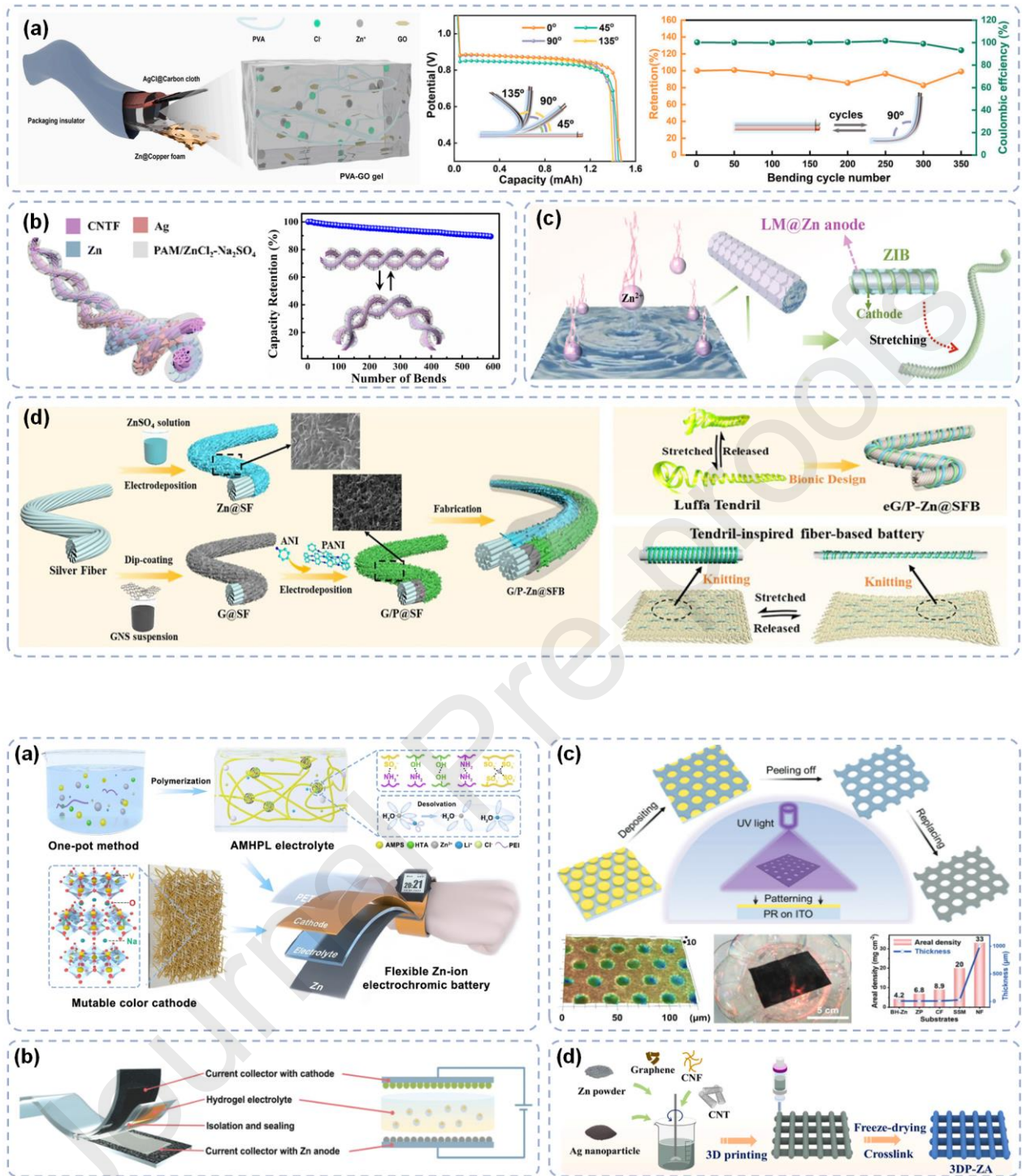


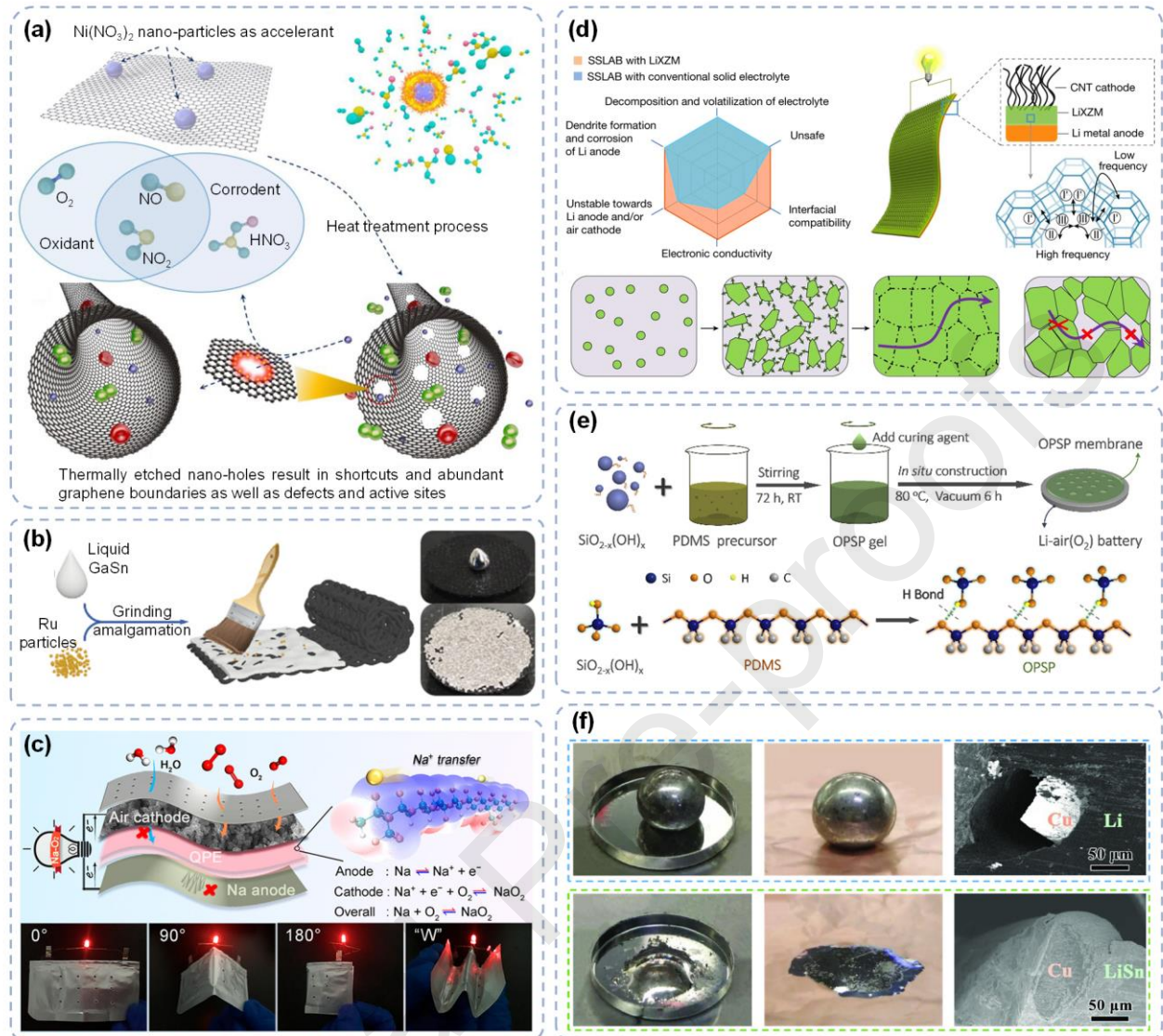
(e) biomass hard carbon

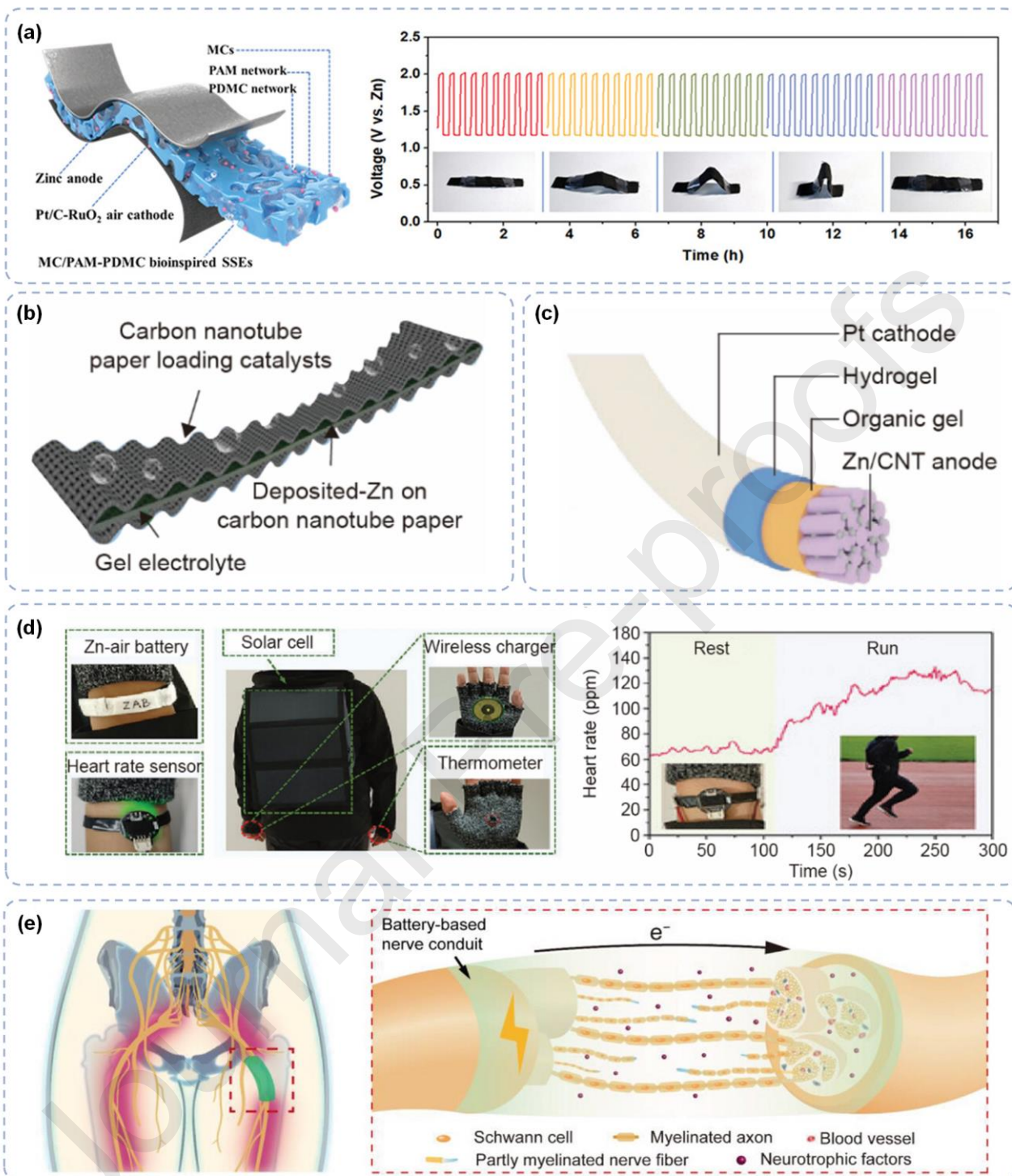
(f) VG/MoSe₂/N-C

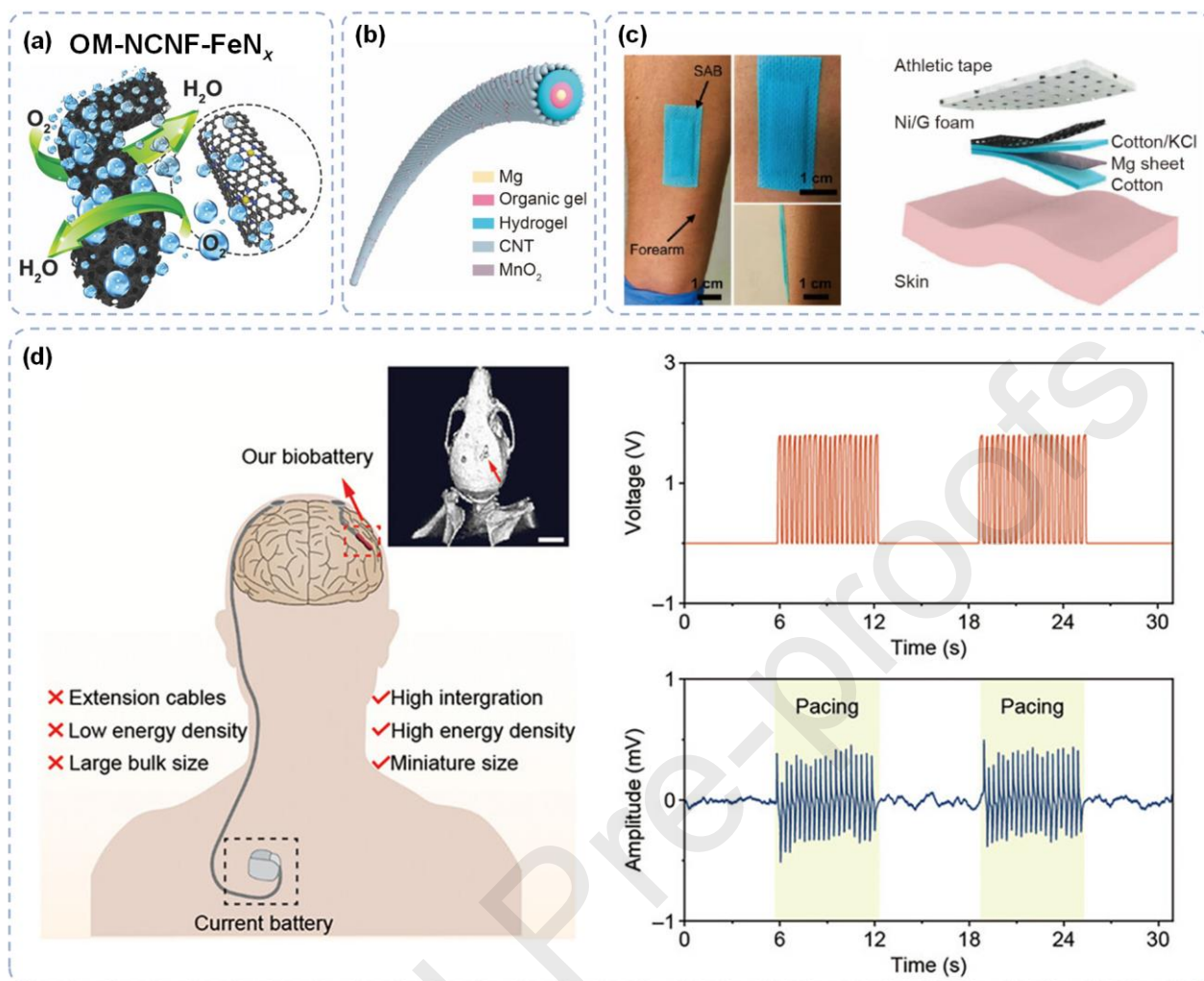
(g) Sn@CNT@carbon paper











This review discusses five distinct types of flexible batteries in detail about their configurations, recent research advancements, and practical applications, including flexible lithium-ion batteries, flexible sodium-ion batteries, flexible zinc-ion batteries, flexible lithium/sodium-air batteries, and flexible zinc/magnesium-

air batteries. Meanwhile, related comprehensive analysis is introduced to delve into the fundamental design principles pertaining to electrodes, electrolytes, current collectors, and integrated structures for various flexible batteries.

Journal Pre-proofs